8-2017

FUNCTIONAL ASYMMETRY OF THE IMMUNE CELL PLASMA MEMBRANE

Eric Malmberg

FUNCTIONAL ASYMMETRY OF THE IMMUNE CELL PLASMA MEMBRANE

By

Eric Malmberg B.S.

APPROVED:

Ilya Levental, Ph.D. Advisory Professor

Yong Zhou, Ph.D.

Mikhail Bogdanov, Ph.D.

Alemayehu Gorfe, Ph.D.

Neal Waxham, Ph.D.

APPROVED:

Dean, The University of Texas

MD Anderson Cancer Center UTHealth Graduate School of Biomedical Sciences

FUNCTIONAL ASYMMETRY OF THE IMMUNE CELL PLASMA MEMBRANE

A

THESIS

Presented to the Faculty of

The University of Texas

MD Anderson Cancer Center UTHealth

Graduate School of Biomedical Sciences

in Partial Fulfillment

of the Requirements

for the Degree of

MASTER OF SCIENCE

By

Eric Malmberg, B.S.
Houston, Texas

August, 2017

Acknowledgements

I would first like to thank my thesis advisor, Dr. Ilya Levental of the UTHealth Graduate School of Biomedical Sciences for his constant support, guidance, and enthusiasm during my graduate studies. His guidance helped me all throughout my research and writing of this thesis and helped make all of this possible.

I would also like to acknowledge the members of my advisory committee: Yong Zhou, Ph.D., Mikhail Bogdanov, Ph.D., Alemayehu Gorfe, Ph.D., and Neal Waxham, Ph.D. Each offered insightful comments, suggestions and hard questions to encourage me to think critically about my project.

I would like to thank my fellow lab mates: Blanca Diaz-Rohrer, Dr. Kandice Levental, Dr. Jupp Lorent, Dr. Hong-Ying Wang, Dr. Lakshmi Ganesan and Shawn Brisbay for their insights, thoughtful discussions and help, and for putting up with me for these two years. You all made research here fun and made it something to look forward to each and every day.

I also want to thank all of my friends here at the UTHealth Graduate School of Biomedical Science in Houston for your continuous support and encouragement.

Finally, I must express my profound gratitude to my parents, Teri and Steve Betz for providing me with unfailing love, support and encouragement throughout all the years. Without their help and encouragement, none of this would have been possible. Thank you.

To my dad, who was in my thoughts throughout this journey. You are missed.

Functional Asymmetry of the Immune Cell Plasma Membrane

Eric Malmberg, B.S.

Advisory Professor: Ilya Levental, Ph.D.

Mammalian cells maintain a distinct disparity in lipid composition between the two leaflets of the bilayer of the plasma membrane. This compositional asymmetry is most prominent for phosphatidylserine (PS), a negatively charged lipid that is found almost exclusively on the cytoplasmic (inner) leaflet of the plasma membrane. This energetically unfavorable asymmetry is maintained by the activity of ATP-dependent transporters called flippases and destroyed by energy-independent lipid channels called scramblases. Although this compositional asymmetry has been known for decades, there has been little investigation of its structural impact on the physical properties of the membrane, nor its functional impact in healthy cells. Here, we seek to determine the effect of compositional asymmetry on the biophysical properties of the plasma membrane and to determine the function of PS scrambling in the activation of immune cells. Canonically, PS is exposed to the extracellular (outer) leaflet of the plasma membrane in an irreversible manner when cells undergo apoptosis, marking them for clearing by macrophages. The primary mediator of PS exposure in cells (otherwise known as phospholipid scrambling) is a calcium activated chloride channel protein known as TMEM16F (or Anoctamin 6; Ano6). The scrambling activity of this channel is gated by intracellular calcium, with increased Ca^{2+} levels leading to channel opening and rapid movement of PS from the inner leaflet to the outer. During cell death and platelet activation, this process is irreversible; however, it has been recently shown that it also occurs in immune cells, but reversibly. Although such behavior has been observed across many different immune cell types, so far, no functional role has been attributed to it. Through pharmacological inhibition and genetic

deletion of Ano6, we show that plasma membrane asymmetry may affect calcium mediated cell signaling in immune cells. This work paves the way for future studies to determine the broad roles of compositional and biophysical plasma membrane asymmetry in cellular physiology, and the specific mechanisms by which it is involved in various cell signaling pathways.

Table of Contents

List of Figures

INTRODUCTION

Almost all mammalian cells have a distinct lipid composition between the two leaflets of the bilayer of the plasma membrane. This compositional asymmetry is most prominent for phosphatidylserine (PS), a negatively charged lipid that is found almost exclusively on the cytoplasmic (inner) leaflet of the plasma membrane(Verkleij et al., 1973). This energetically unfavorable asymmetry is maintained by the activity of ATP dependent transporters called flippases(Shor et al., 2016). Canonically, PS is exposed to the extracellular (outer) leaflet of the plasma membrane when cells undergo apoptosis. This exposure marks dead cells for phagocytosis by macrophages, which detect the exposed PS on the plasma membrane(Ravichandran, 2010). PS exposure also occurs in platelets upon activation, where it is an essential component of the clotting cascade; PS exposure is essential for assembly of fully active prothrombinase complexes(Rosing et al., 1980). This PS exposure has been shown to be mediated by membrane bound scramblase proteins, such as those in the anoctamin family or the Xkr family(Nagata et al., 2016). The anoctamin scramblase family contains 10 members, which carry multiple transmembrane domains(Gyobu et al., 2016). Most are located at the plasma membrane, where 5 of these family members function as a calcium dependent phospholipid scramblase(Suzuki et al., 2013). Among the more prominent of these is Anoctamin 6 (Ano6), a recently identified calcium activated chloride channel protein and the primary mediator of PS exposure in cells(Whitlock and Hartzell, 2017). The scrambling activity of this channel is gated by intracellular calcium, with increased intracellular calcium levels leading to activation and rapid movement of PS from the inner leaflet to the outer(Oh and Jung, 2016).

Although it has not been fully demonstrated, this scrambling is not believed to be specific to PS, but rather most lipids in the PM can redistribute according to their concentration gradients, thus destroying the asymmetry of the living cell PM. Canonically, this loss of PS asymmetry was believed

to be irreversible, occurring during cell death(Nagata et al., 2016) or during platelet activation as an active component of the clotting cascade(Bevers and Williamson, 2010). However, it has been recently shown that it also occurs in immune cells in a transient manner(Martin et al., 2000). Here, Ca^{2+} spikes induced by immune receptor activation induce transient PS exposure, which is then rectified by the activity of flippases(Devaux, 1988). Mutations in Ano6 have been shown to be implicated in the rare congenital bleeding disorder known as Scott Syndrome(Zwaal et al., 2004). This disorder is characterized by instances of severe and uncontrollable bleeding. Patients exhibiting this syndrome show platelet cells that are incapable of externalizing PS during the activation of the clotting cascade(Zwaal et al., 2004). During this cascade, phospholipids and calcium facilitate the binding of FXa and FIXa to the surface of platelets(Spronk et al., 2014). Because platelet cells in patients with Scott Syndrome are unable to externalize PS during the activation of this clotting cascade, platelet cells are unable to bind FXa and FIXa, leading to a cessation in the clotting cascade followed by uncontrollable bleeding(Rosing et al., 1985). The findings from patients with Scott Syndrome implicate a potential functional role of PS during periods of intracellular calcium flux, and may offer new insights into a potential functional role of plasma membrane asymmetry. The loss of this asymmetry has been shown to occur in a transient manner during periods of normal cell signaling, such as what occurs during immune cell activation(Segawa et al., 2011).

Although such behavior has been observed across many different immune cell types(Smrž et al., 2007), and there are indirect indications that PS exposure may be functionally important for immune cell function, the specific functional roles are not well understood, nor are the cellular mechanisms affected by PS scrambling in healthy cells. We hypothesize that **active PS scrambling changes the biophysical properties of the plasma membrane, thereby affecting cell signaling during activation**. We addressed this hypothesis through the following aims: 1) to determine the

effect of PS asymmetry on the biophysical properties of the plasma membrane and 2) to determine the functional role of PS scrambling during immune cell signaling.

We addressed the effect of PS asymmetry on the biophysical properties of the plasma membrane using the giant plasma membrane vesicle (GPMV) model system (fig1-A), a novel technique to isolate and analyze native plasma membranes from intact cells. This method involves chemically induced blebbing of the membrane away from live cells by a treatment containing sulfhydryl-reactive chemicals in a calcium-containing buffer. The PM vesicles formed by this procedure contain the native complexity and diversity of intact cell PMs(Sezgin et al., 2012). Remarkably, these isolated PMs also phase separate into macroscopic, coexisting liquid domains (Fig 1-A). These domains have different compositions and physical properties, similar to the coexistence of liquid disordered and liquid ordered domains in synthetic model membranes(Veatch and Keller, 2003). Although we cannot see large rafts in living cells, these GPMVs are the best proxy for studying this behavior in a biological system. Because of their biological origin, these intact PM vesicles contain the complexity and diversity of native membrane components, making them an excellent model system to study plasma membrane biophysical properties. Furthermore, the liquid-liquid phase separation therein provides compelling evidence for the central tenant of the lipid raft hypothesis(Levental and Levental, 2015). Methodologically, this model system offers great insights into the biophysical nature of the native state plasma membrane allowing for the investigation of structural determinants of raft partitioning,

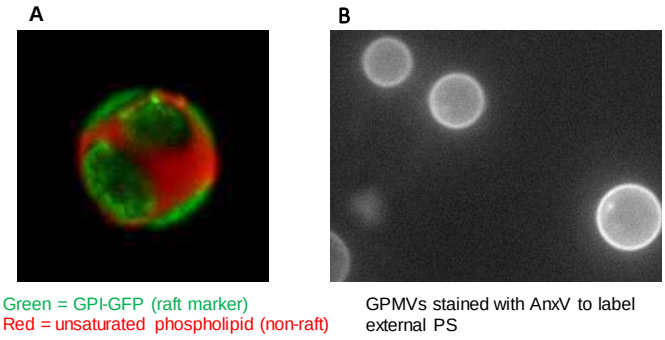

Figure 1: GPMVs as a model system to study the plasma membrane A) GPMVs can partition into liquid ordered and liquid disordered phases, each of which can be labeled with raft or non-raft markers. GPMVs are also useful in studying the biophysical properties of the PM. **B)** Unlike native state PMs, PS is externalized during GPMV formation. This is the most significant limitation to GPMV as a model system to study the PM

protein distribution (liquid order or liquid disorder) and how this partitioning can affect cell signaling(Sengupta et al., 2008; Simons and Toomre, 2000). GPMVs can also be used to determine the lipid content of the PM in response to a variety of conditions including growth, temperature, stress, etc(Burns et al., 2017). However, these GPMVs are not fully representative of the native state of living plasma membranes, in that PS is externalized in these vesicles, as shown in Figure 1-B. Here, a calcium dependent phospholipid binding protein, Annexin V (AnxV) was used to label externalized PS during GPMV formation. This loss of asymmetry is one of the more significant limitations to accurately studying the various biophysical properties of the natively asymmetric plasma membrane. The method required for the production of GPMVs requires the use of chemicals that may make the plasma membrane permeable to ions such as calcium(Keller et al., 2009) (which is required for the production of GPMVs). We hypothesized that this increase in intracellular calcium during GPMV formation activates the calcium dependent PS scramblase Ano6, thereby actively inducing PS exposure. For the experiments in Aim 1, we explored ways to produce PS asymmetric GPMVs using a variety of inhibitor and genetic tools that target the calcium activated scramblase protein, Ano6.

The second aim of this project is to determine the function of PS scrambling during the activation of immune cell signaling. Although PS scrambling is canonically believed to be an irreversible process, used as an “eat me” signal to macrophages(Ravichandran, 2010), recent studies have suggested that in healthy cells, PS externalization is transient and can occur during periods of intracellular calcium spikes(Smrž et al., 2007). This PS externalization has also been suggested to be

mediated by the calcium activated chloride channel scramblase, Ano6(Ousingsawat et al., 2015). We evaluated the functional role of PS asymmetry during immune cell signaling (degranulation, Fig 2), utilizing rat basophilic leukemia cells (RBLs) as a model system. These cells function similarly to mast cells, in that they can undergo antigen-mediated exocytosis of intracellular granules(Barsumian et al., 1981). Mast cells are part of the innate immune system, which is involved in phagocytic action and pathogen killing activity(Singh et al., 2016). Mast cells are retained in close vicinity with blood vessels, which allows them to have a crucial sentinel role in host defense(Marshall, 2004). These cells contain a variety of functions including regulation of both innate and adaptive immunity(Singh et al., 2016), tolerance to skin graft rejection(de Vries and Noelle, 2010), among many others. They play a pivotal role in protective immunity, including the ability to respond to and inactivate venoms, such as those from a honey-bee and viper(Galli et al., 2016). However, they are also implicated in various allergic reactions, including anaphylactic shock(Zhou et al., 2013). The classical form of allergic reaction involves mast cell degranulation to release histamines in response to antigen, leading to the mobilization of a variety of inflammatory signals(Theoharides et al., 2012).

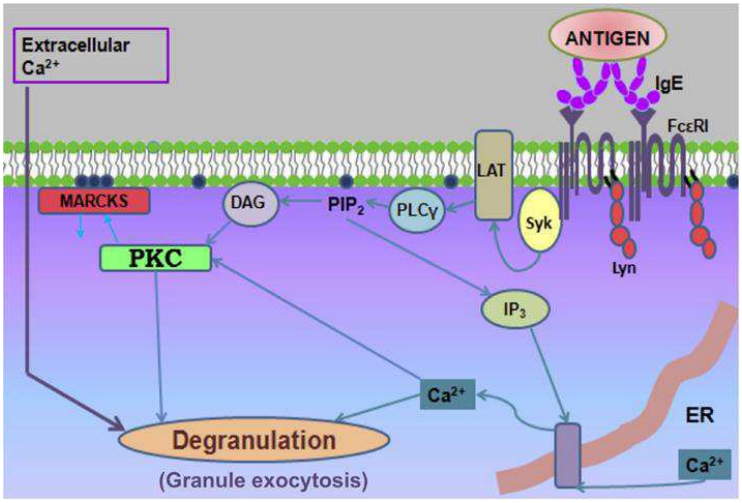

Figure 2: Schematic diagram of the degranulation pathway in mast cells. Binding of antigen (via IgE) to receptors on the cell surface activates signaling pathways, resulting in activation of PKC and release of intracellular calcium, which in turn leads to exocytosis of histamine-containing granules. The increase in intracellular calcium may also activate Ano6, which is involved in the scrambling and externalization of PS. Figure as originally published with permission from Holowka, D., Wilkes, M., Stefan, C., and Baird, B. (2012). Front. Immun. doi:10.3389/fimmu.2012.00104

In mast cells, histamine granule exocytosis is initiated by antigen binding and crosslinking IgE, which is in turn bound to transfer Fc receptors. This crosslinking results in a signaling cascade leading

to the mobilization of intracellular calcium, activation of PKC and the release of granules containing histamines and enzymes(Holowka et al., 2016). We hypothesize that the mobilization of intracellular calcium during the degranulation process leads to the activation of Ano6, resulting in a loss of PM asymmetry by externalization of PS. This loss of asymmetry may be functionally important to the progression of the degranulation pathway, and may affect mast cell function. In order to address this hypothesis, we investigated PS exposure during Ca^{2+}-mediated signaling and the mechanism for how lipid scrambling of the PM may affect immune cell activation by targeting a Ca^{2+}-activated Cl^- channel scramblase protein and evaluated the degranulation efficiency in a mast cell line.

RESULTS

Chemical inhibition of scramblase in plasma membranes produces PS-asymmetric GPMVs.

The primary mediator of PS scrambling in healthy cells is a recently identified scramblase protein Anoctamin 6 (Ano6), a calcium activated chloride channel protein found in nearly all eukaryotic cells(Martins et al., 2011). It has been found to be necessary and sufficient to mediate rapid movement of PS from the inner to the outer leaflet of the PM(Whitlock and Hartzell, 2017). Fig 3 depicts the proposed mechanism of action of Ano6. Ca^{2+} binding causes a conformational change in Ano6, which allows for flux of Cl^- ions and exchange of lipids between the inner and outer leaflet of the PM. Ano6 can be inhibited chemically, using a Ca-activated chloride channel blocker known as A01 (6-(1,1-Dimethylethyl)-2-[(2-furanylcarbonyl)amino]-4,5,6,7-tetrahydrobenzo[*b*]thiophene-3-carboxylic acid).

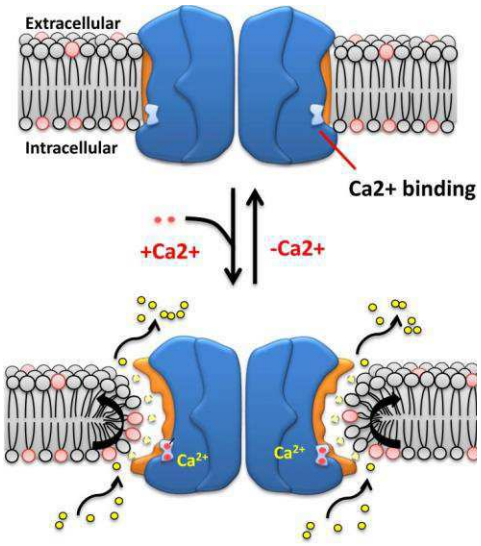

Figure 3: Schematic of Ano6 mediated PS scrambling. Ca^{2+} binding opens a cavity that allows the exchange of ions and phospholipids between leaflets. Figure as originally published with permission from Oh, U., and Jung, J. (2016). Eur. J. Physiol. doi: 10.1007/s00424-016-1790-0

In an attempt to produce native PS-asymmetric GPMVs, 150uM A01 was added to the GPMV production buffer and PS exposure to the outer leaflet was measured using binding of a fluorescently tagged Annexin V (tagged with Alexa568; AnxV-568). While control GPMVs clearly and strongly bound AnxV-568, A01 treatment produced GPMVs that did not show obvious AnxV binding (not shown), suggesting that PS remained on the internal leaflet. Because such microscopic assays are difficult to

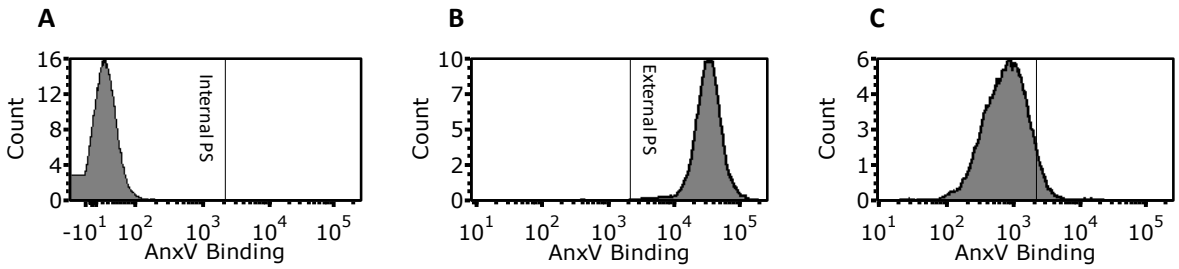

Figure 4: A01 inhibits PS exposure in GPMVs. Flow cytometry data of **(A)** unlabeled GPMVs (i.e. background fluorescence); **(B)** control GPMVs labeled with AnxV show high AnxV binding to nearly all vesicles, revealing externalization of PS; **(C)** GPMVs produced in the presence of A01. A01 successfully inhibits PS externalization during GPMV formation.

quantitate and do in high-throughput, we verified that A01 GPMVs were PS-asymmetric by using flow cytometry to measure AnxV568 binding (Fig. 4). Vesicles produced in the presence of A01 show minimal AnxV binding, indicating a lack of exposed PS, verifying PS-asymmetric GPMVs.

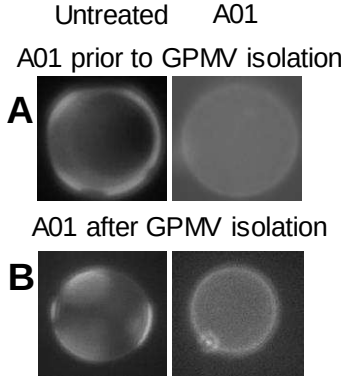

Figure 5: A01inhibits phase separation in GPMVs A) GPMVs isolated using standard conditions show macroscopic phase separation below ~15°C. A01 inhibits phase separation when added during GPMV isolation **B)** A01 inhibits phase separation when added after GPMV isolation

Having produced PS-asymmetric GPMVs, we next sought to answer our central question of whether lipid asymmetry affected PM physical properties. Specifically, we assayed whether asymmetry affects domain formation by analyzing phase separation of vesicles produced with A01. GPMVs produced with A01 showed a dramatic reduction in phase separation compared to untreated vesicles. At temperatures as low as 2°C, there was no observable phase separation in GPMVs produced with A01, in contrast to control GPMVs, where phase separation could be observed as high as 15°C (Fig 5-A). This observation suggested that PS asymmetry had a major effect on phase separation in isolated PMs, essentially completely suppressing phase separation. However, we needed to control for a possible non-specific effect of the A01 compound itself, rather than its effect on asymmetry. To that end, we added A01 to

GPMVs after isolation, which should not have any effect on PS asymmetry, which had been lost during isolation in the absence of drug. This treatment also resulted in a wholesale abolition of phase separation, similar to addition of A01 prior to GPMV isolation, despite having no effect on PS asymmetry (Fig 5-B). These observations revealed that A01 directly impacts membrane biophysical properties independent of its effect on PS asymmetry. To separate the direct effects of A01 from its effects on PS asymmetry, we attempted several means to wash out the drug after isolation of PS asymmetric GPMVs. The protocol for monitoring efficiency of wash-out was as follows: A01 was added to GPMVs (final concentration 50uM), which lead to a loss of phase separation observed via fluorescence microscopy at 10°C. We hypothesized that successful removal of A01 from GPMVs would produce a return of microscopically observable phase separation.

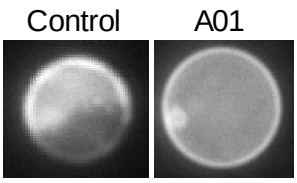

Figure 6: Dialysis of GPMVs after addition of A01. A01 was added to GPMVs after production and isolation, followed by dialysis in GPMV buffer overnight at 4C. There was no return of phase separation in GPMVs after this dialysis.

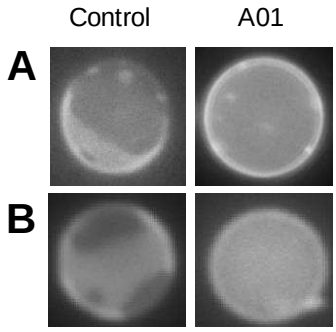

Figure 7: Failure to remove A01 from GPMVs. A) GPMVs dialyzed overnight at 4°C in GPMV buffer containing Bio-Beads. No return of phase separation suggested failure to remove the drug. **B)** An excess of synthetic SUVs was added to GPMVs after production in an attempt to dilute A01. There was no return of phase separation in these GPMVs.

The first attempt to wash-out A01 was by dialysis. Vesicles were dialyzed in GPMV buffer (150mM NaCl, 2mM $CaCl_2$, 10mM HEPES pH7.4) for 2hr, 4hr or overnight at 4C. None of these protocols produced an observable return of phase separation after dialysis (Fig 6). We then attempted to wash-out A01 using Bio-Beads, which are designed to remove detergents and other lipophilic materials from solutions. GPMVs treated with A01 were dialyzed in a solution containing these beads for 2hr, 4hr or overnight at 4C. Again, there was no observable phase separation in GPMVs dialyzed with Bio-Beads (Fig 7A). Finally, we tried incubating with small unilamellar

vesicles (SUVs) to remove A01 from GPMVs. Since A01 is slightly lipophilic, we hypothesized that it was incorporating into membranes non-specifically, though not necessarily irreversibly. Thus, we reasoned that SUVs would provide a large pool of membranes, thereby effectively diluting the drug

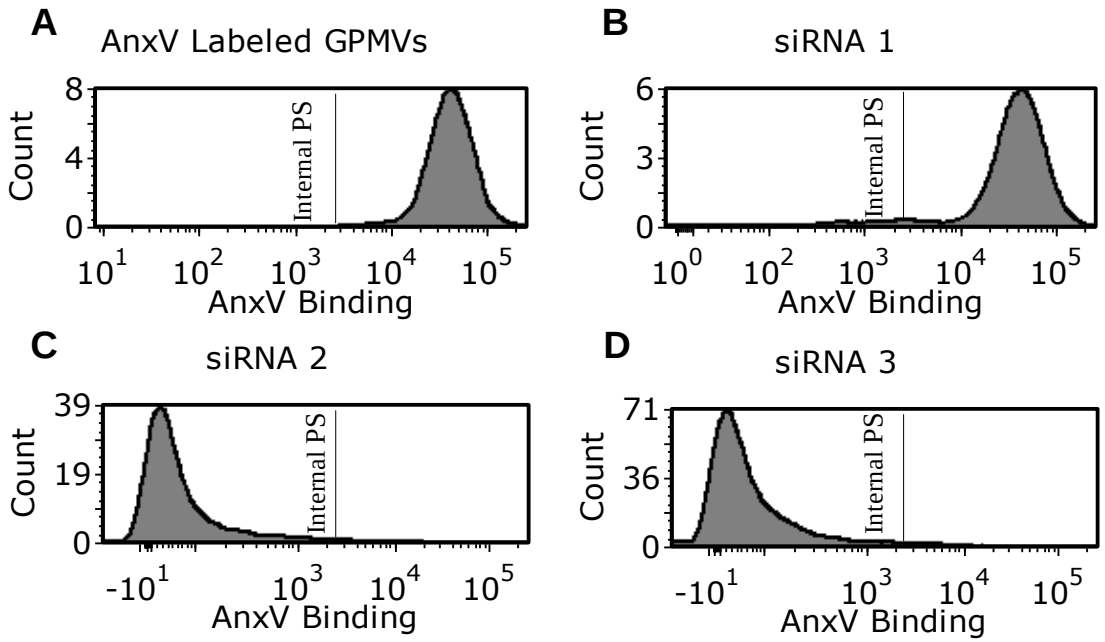

Figure 8: GPMVs produced from Ano6 knockdown are PS asymmetric. A) Flow cytometry showing AnxV binding to control GPMVs, indicating externalization of PS. **B)** Although siRNA 1 was unable to knockdown Ano6, **C-D)** a large subset of GPMVs prepared after siRNA knockdown of Ano6 with siRNA 2 and 3 did not bind AnxV, thus remained PS-asymmetric. Data obtained by Barbara Diaz-Rohrer

from the GPMVs. Unfortunately, as in all other wash-out experiments, we did not observe a recovery of phase separation, leading us to abandon these attempts to remove A01 from GPMVs (Fig 7B).

siRNA knockdown of scramblase protein Ano6 to produce PS asymmetric GPMVs.

Although the chemical inhibition of Ano6 produced PS asymmetric GPMVs, A01 dramatically affected phase separation independent of its effect on PS asymmetry. Thus, this artifact prevented analysis of the biophysical properties of PS asymmetric membranes using A01 for isolation. To overcome this limitation, we attempted to produce asymmetric GPMVs by removing, rather than inhibiting, Ano6. The first step was to determine if removing Ano6 in cells would result in the

production of PS asymmetric GPMVs. To this end, we used siRNA targeting Ano6 in Rat Basophilic Leukemia (RBL) cells to knock down the levels of this protein and test the effect of PS asymmetry in isolated GPMVs. Cells were transfected with one of three siRNA sequences targeting Ano6, or a combination of all three. 2 days after transfection, GPMVs were produced from these cells, and external PS was labeled using AnxV, which was quantified by flow cytometry. Fig 8 indicates that all siRNA treatments resulted in the production of a subset of GPMVs that appeared to have PS remaining internal. Most notably, sequences 2 and 3 (see materials) lead to near-complete abolition of PS externalization. These results confirm that targeting of Ano6 in RBLs is a promising direction for production of PS asymmetric GPMVs.

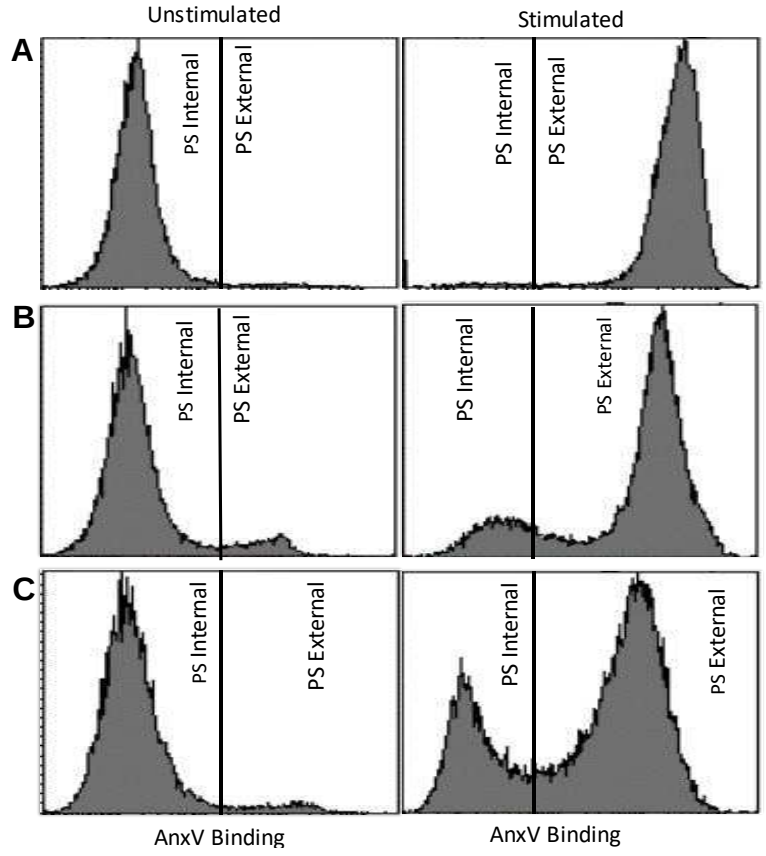

Figure 9: Flow cytometry of RBL cells transfected with CRISPR plasmids targeting Ano6. Plasmids contain two different gRNA sequences (labeled Cas9-1 or Cas9-2 respectively), followed by treatment with ionomycin and AnxV-568 to label external PS. **A)** Cells transfected with an empty Cas9 plasmid robustly externalized PS upon treatment with 5uM ionomycin (5min; 37C). **B-C)** Cells transfected with CRISPR plasmids targeting Ano6 showed clear increases in the number of cells that did not externalize PS upon calcium flux mediated by ionomycin.

Knockout of Ano6 in RBLs using CRISPR/Cas9 produces cells which do not externalize PS during ionomycin mediated calcium stimulation.

Although siRNA treatment was successful in producing PS asymmetric GPMVs RBLs have a very low transfection rate (~30%). We determined that producing a complete Ano6 knockout cell line

would allow for more consistent results during each experiment, removing the potential error of transfection inefficiency. To produce an Ano6 KO cell line with RBLs, we utilized the CRISPR/Cas9 system, targeting exon 6 of Ano6. Two gRNA sequences were used and cells transfected with the CRISPR plasmid (PX458). In order to show that knockout of Ano6 using CRISPR/Cas9 was successful in inhibiting PS externalization, PS externalization during ionomycin-mediated calcium stimulation was analyzed using flow cytometry. Ionomycin is an ionophore, used to raise the levels of intracellular levels of calcium. Fig 9 shows that CRISPR targeting of Ano6 was successful in producing a population of cells that do not externalize PS during ionomycin mediated calcium stimulation (as shown by a lack of AnxV binding).

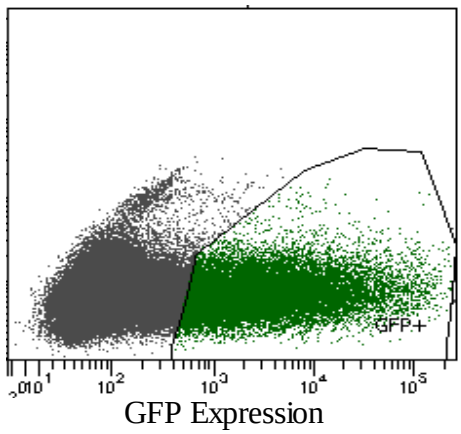

Figure 10: Sorting of RBL cells based on GFP expression. The CRISPR/Cas9 plasmid used contains a GFP reporter gene, which is used to show successful transfection into a cell. Cells expressing GFP were kept, while the cells not expressing GFP were discarded

After verifying that the CRISPR targeting of Ano6 lead to the expected/desired phenotype (no externalization of PS during calcium flux induced by ionomycin), another batch of cells were transfected and sorted using fluorescence activated cell sorting (FACS). These cells were bulk sorted for expression of the CRISPR plasmid, which contained a reporter GFP (Fig 10). After recovery, cells were treated with ionomycin, external PS was labeled with AnxV, and AnxV binding was analyzed via flow cytometry, showing a large percentage of cells with an Ano6 KO phenotype (i.e. not exposing PS upon ionomycin treatment) (Fig11A).

While this approach was successful in generating cells, which did not expose PS upon calcium stimulation, it did not produce a pure population of such cells. We initially presumed this was because not all transfected (i.e. GFP-positive) cells produced an effective CRISPR knockout. To isolate only those cells which did not expose PS, the GFP-sorted population from Fig 11A cells were further sorted by FACS using the desired phenotype of minimal ionomycin-stimulated AnxV binding. After recovery, these sorted cells were analyzed using ionomycin and AnxV binding to determine if this protocol produced a pure population of cells that failed to externalize PS. Surprisingly, as shown in Fig11B, while the phenotype-directed sorting yielded a large population of cells that did not externalize PS upon ionomycin mediated calcium stimulation, it was far from complete (~50%). Even

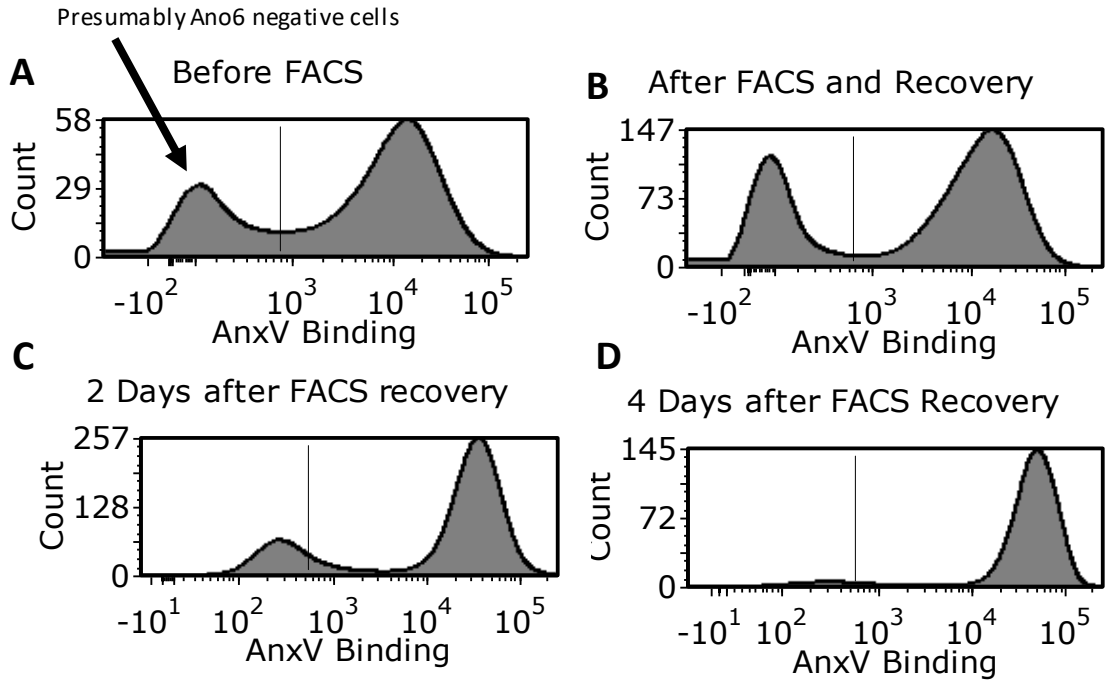

Figure 11: CRISPR targeting of Ano6 produces RBLs that do not externalize PS during ionomycin mediated calcium stimulation, but not stable lines. (A) Flow cytometry analysis of AnxV binding (i.e. PS exposure) following ionomycin stimulation in RBL cells sorted by GFP expression after transfecting with CRISPR plasmid targeting Ano6. This protocol produced a significant – though incomplete – population of cells that did not externalize PS. **B)** Cells that did not externalize PS were further sorted, based on lack of AnxV568 binding upon ionomycin mediated calcium stimulation. After sorting, this population of cells was further analyzed for ionomycin-mediated PS exposure. The proportion of cells that did not externalize PS increased notably, but still not nearly to 100%. **C)** Two days after the analysis in B, the population of cells that did not externalize PS upon ionomycin mediated calcium stimulation decreased dramatically and **D)** essentially disappeared four days after the initial sort.

more surprisingly, two days after this initial analysis, the population of cells that did not externalize PS dramatically decreased (Fig 11C), and four days after the initial analysis this population of cells had nearly completely disappeared (Fig 11-D). This disappearance of the AnxV-negative population suggested that these cells were at a growth disadvantage compared to the WT RBLs.

To prevent Ano6 KO cells from being at a growth disadvantage compared to the WT RBLs, single cell cloning of CRISPR/Cas9 Ano6 KO cells was also attempted. Using FACS, single cells expressing GFP (an indicator of successful CRISPR transfection) were sorted into individual wells of a 96-well dish. After sufficient colony expansion, we sequenced the genomic region targeting Ano6 to determine if clonal colonies were genetically modified by CRISPR/Cas9. All single-cell clones that grew into large colonies had the wild type Ano6 sequence, indicating no CRISPR-mediated modification. However, there were a number of wells that remained single cells for one month; the cell was healthy but did not divide. This single cell cloning was attempted multiple times, using both gRNA sequences, by multiple experimenters, all with the same results. From this set of observations, we concluded that Ano6 may be an essential gene for cell division in RBLs, and therefore that stable knockouts cannot be produced. RBLs may not have been the optimal choice for producing an Ano6 KO cell line, as they may be lacking in other anoctamin family members, which may be required for cell survival(Suzuki et al., 2013). Moving forward, we switched to using a new cell line to produce an Ano6 knockout in HeLa.

Development of Ano6 KO HeLa cell line.

Due to the insuperable hurdles encountered in our attempts to develop an Ano6 KO cell line in RBLs, we switched our focus to developing an Ano6 KO cell line in HeLa cells. These cells were selected in part due to the ease of transfecting compared to RBLs (20-30% efficiency in RBLs) and also because they may express other Ano6 family members that could support cell survival in the absence of Ano6. HeLa cells were treated exactly like RBLs – i.e. transfected using the same CRISPR/Cas9 plasmid, but containing an established gRNA sequence targeting exon 6 in Ano6 (see methods). For this attempt, we did not attempt to establish a bulk-sorted population, but rather tried immediately for single-cell clones. Genomic DNA from these clones was sequenced to determine whether Ano6 KO was successful. Two clones were identified which showed frame-shift mutations - one a single base pair insertion (KO4) and the other containing an insertion-deletion (KO1) (Fig 12). Knockout was next validated using Western Blotting (Fig 13) indicating that both knockouts were not producing the Ano6 protein and flow cytometry (Fig 14). For flow cytometry analysis, WT and KO cells were treated with ionomycin to increase intracellular calcium levels, activate Ano6, and induce PS scrambling. This flow cytometry data supports the genetic and Western blotting evidence,

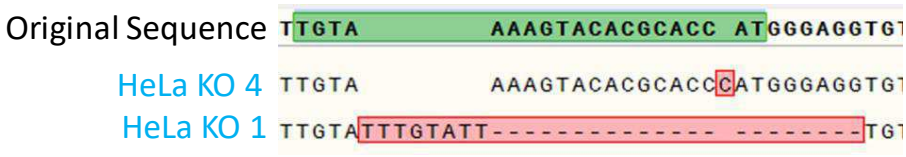

Figure 12: CRISPR/Cas9 targeting of Ano6 in HeLa produced two Ano6 KO clones. Genomic DNA of HeLa clonal colonies produced by transfecting the parental cells with a CRISPR/Cas9 plasmid targeting Ano6. Clone KO4 contained a single base-pair insertion, while clone KO1 contain an insertion-deletion mutation. Both are non-sense mutations expected to lead to protein knockout.

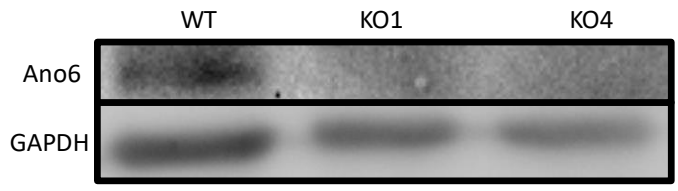

Figure 13: Western Blot of Ano6 in HeLa Ano6 KO clones. Ano6 is not produced in either HeLa KO clone, as indicated by Western Blot analysis.

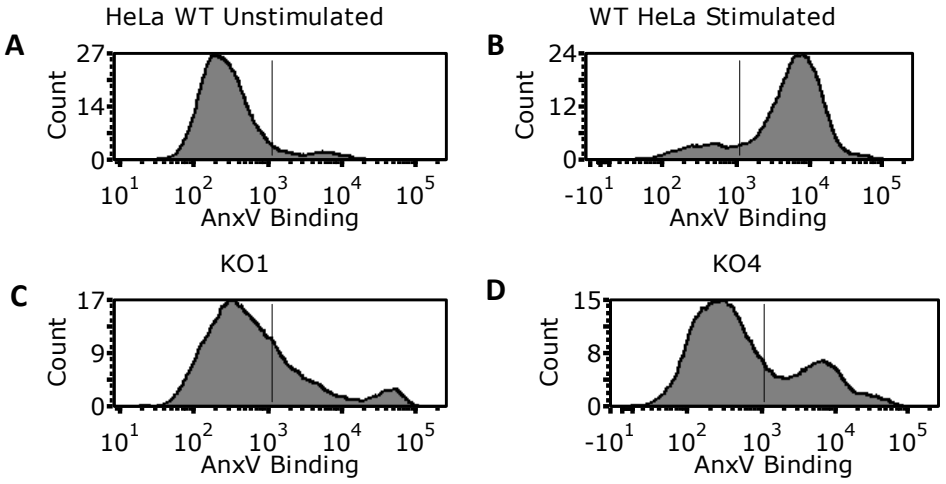

Figure 14: Ano6 knockout HeLa clones do not externalize PS upon ionomycin mediated calcium stimulation. A) Unstimulated HeLa cells do not externalize PS. **B)** Ionomycin treatment results in robust PS externalization in WT HeLa cells. **C)** KO1 and **D)** KO4 clones contained large populations of cells with impaired PS externalization, as expected from Ano6 knockout. Although the majority of cells are AnxV-negative, there is a small population of AnxV-positive cells. These could be residual WT cells remaining from the cloning procedure, or knockouts that externalize PS by other mechanisms.

indicating that Ano6 knockout in HeLa cells was successful in producing cells that do not externalize PS upon ionomycin mediated calcium stimulation. There also appears to be a population of HeLa's that do externalize PS. These could be residual WT cells remaining from the cloning procedure, or knockouts that externalize PS by other mechanisms.

Isolation of GPMVs from Ano6 KO cells.

Having verified successful knock-out of Ano6 in HeLa, and that these cells exhibited the expected phenotype during ionomycin mediated calcium stimulation (lack of PS externalization), we sought to isolate GPMVs from these cells. The rationale being that since these cells are resistant to PS scrambling upon calcium influx, their GPMVs would remain asymmetric. GPMVs were produced using standard protocols (specifically the PFA/DTT isolation), and external PS was labeled using fluorescent AnxV. AnxV binding was quantified in fluorescent images by drawing line-scans through each vesicle in ImageJ. The fold intensity over background fluorescence was then used as a semi-quantitative readout of AnxV binding for each vesicle.

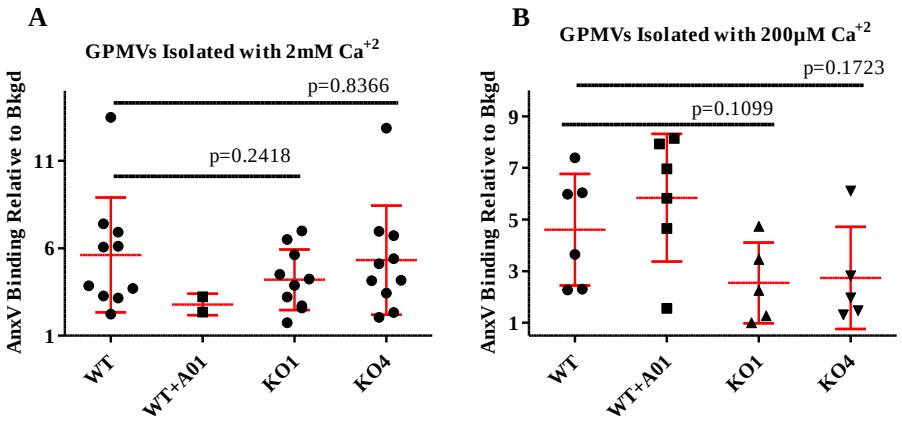

Figure 15: AnxV labeling of GPMVs produced from HeLa Ano6 KO cells. **A)** GPMVs produced from WT HeLa cells and Ano6 KO lines in the presence of 2mM calcium. A01 treatment of cells prior to GPMV isolation leads to a significant decrease in AnxV binding, as expected (see Fig 3A). While both KOs showed slightly reduced AnxV binding compared to WT, the effects were highly variable and not statistically significant. **B)** Similar results were observed in vesicles prepared using 200 µM Ca^{2+} for GPMV isolation. The only notable difference was that A01 slightly increased AnxV binding, which was an unexpected and unexplained observation. Error bars: Standard error of mean

We compared this per-vesicle intensity between GPMVs isolated from WT HeLa cells and KO1 and KO4 clones. GPMVs produced with A01 (150uM) was used as a positive control for impaired PS externalization / AnxV binding. Although there appeared to be a decrease in AnxV binding in Ano6 knockout clones compared to WT, there was significant experiment-to-experiment variability. In two experiments (out of ten), the result was perfect – i.e. no measurable AnxV binding to GPMVs from clones, robust binding in WTs. However, in the other experiments, the results were less robust, with occasional experiments showing no difference at all between WT and KOs (Fig 15-A). Ultimately, statistical analysis of all experiments showed no low p-values (WT and KO1 p=0.2418, WT and KO4 p=0.8366) and therefore no confident statistical statement could be made about the difference between the groups. To date, we have been unable to find the source of this experimental variability, and therefore currently cannot consistently produce asymmetric GPMVs.

Ca^{2+} levels were altered during GPMV formation.

To explain these observations, we hypothesized that the large concentration of Ca^{2+} (2mM) used in GPMV isolation may be responsible for activation of other potential Ca^{2+}-activated scramblase

proteins within the cell. To address this, we determined the minimum concentration of Ca^{2+} that could be sufficient to produce an appropriate number of GPMVs, and determined this value to be ~200 μM. We produced GPMVs with this lower calcium level and analyzed in the same manner as described above. Unfortunately, the overall variability of AnxV binding was not reduced and there was still not significant difference between the groups (Fig15-B WT and KO1 p=0.1099, WT and KO4 p=0.1723). It is surprising to note that AnxV binding in the positive control group (WT + A01) appear to be much greater than the negative control (WT). We currently do not have an explanation for this effect. Nevertheless, these results indicate that lower concentrations of Ca^{2+} during GPMV formation, in either WT HeLa or Ano6 knockouts, did not yield PS asymmetric GPMVs.

There are other TMEM16 (Anoctamin) scramblase proteins that may be involved in PS scrambling during GPMV formation.

It is possible that the inability of HeLa Ano6 knockouts to produce PS asymmetric GPMVs may be the result of scramblase activity from other anoctamin family proteins not expressed in RBLs. There is a total of 9 additional Anoctamin proteins in eukaryotic cells, 5 of which have been shown to exhibit scramblase activity(Suzuki et al., 2013). In tissues associated with immunity, it was shown that the only Anoctamin scramblase protein expressed is Ano6 (TMEM16F). However, in ovary and uterine tissues, Ano6 is the most abundantly expressed scramblase protein, but others are present as well, namely Ano4 and Ano9 (TMEM16D and J, respectively). If true in HeLa, the presence of these scramblase proteins (Ano4, Ano9) may be compensating for the loss of Ano6 in HeLa KOs, resulting in the loss of PS asymmetry during GPMV formation.

Caspase-3 is activated during GPMV formation.

There are also other non-TMEM scramblase proteins, one of which is Xkr8 (XK related 8 protein), and it is activated by apoptosis(Suzuki et al., 2014). Active caspase-3 has been shown to activate this protein in response to apoptotic stimuli, and the mechanism of scrambling is independent of Ca^{2+} induced PS exposure by the TMEM family members. We postulated that GPMV formation is leading to the activation of apoptotic pathways in cells, specifically the activation of caspase-3.

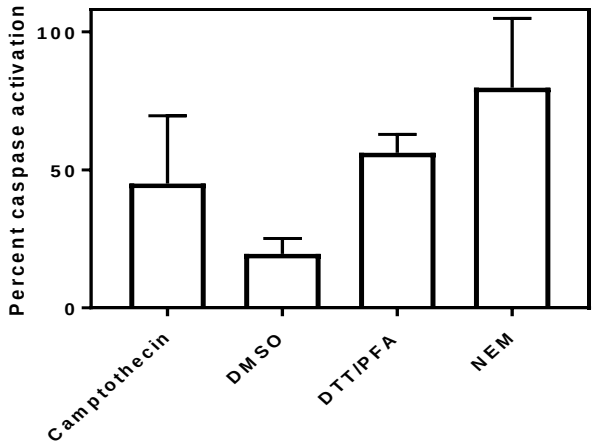

Figure 16: Percentage of HeLa cells with active caspase following a variety of treatments. Cells were treated with camptothecin as a positive control to induce apoptosis, or with GPMV buffer for 45min at 37C, followed by labeling with a caspase 3/7 detection reagent. These results indicate that apoptotic caspases are being activated during GPMV formation, which potentially activates Xkr8.

In order to test whether caspase-3 was activated during GPMV formation, cells were treated with a known inducer of apoptosis as a positive control (10 μM camptothecin 8 h at 37°C) or buffers used to produce GPMVs (containing DTT/PFA or NEM) under standard GPMV isolation conditions (37°C for 45 min). After this incubation period, caspase-3 activation was detected by addition of a caspase-3/7 detection dye (see methods). This dye is cleaved only by active caspase-3 and 7, resulting in the release of a fluorescently tagged molecule that binds to nuclear DNA, such that cells with active caspase-3 present with brightly fluorescent nuclei. Results from these experiments (Fig. 16) indicate that production of GPMVs using NEM or DTT/PFA in a calcium containing buffer results in the activation of caspase-3/7, to a level even above camptothecin. The activation of caspase-3 during GPMV formation suggests a mechanism by which PS may be externalized in Ano6 KO HeLa cells, i.e. via activation of the apoptotic scramblase protein Xkr8.

Z-DEVD-fmk was used to prevent caspase-3 activation.

To prevent the activation of caspase-3 during GPMV formation (and potentially prevent activation of PS scramblase Xkr8), we attempted to use Z-DEVD-fmk, a known irreversible inhibitor of caspase-3. Cells were pre-treated for one hour with Z-DEVD-fmk (100 μM) in growth medium, followed by treatment with GPMV buffer (supplemented with DTT/PFA or NEM) containing Z-DEVD-fmk (100 μM) for 45 min. As a control to validate that Z-DEVD-fmk inhibits caspase-3 activation, cells were treated with camptothecin (10μM 8 h at 37°C) containing 100uM Z-DEVD-fmk. Caspase-3 activity was measured using a caspase-3/7 detection dye (Thermo). Surprisingly, although Z-DEVD-fmk is capable of preventing activation of caspase-3 in the camptothecin control, it is unable to prevent caspase-3 activation during GPMV formation with DTT/PFA (Fig 17). Inhibition of caspase-3 was attempted during NEM mediated GPMV formation, with similar results as observed in DTT/PFA produced GPMVs, i.e. no effect of the inhibitor on caspase-3 activation (not shown).

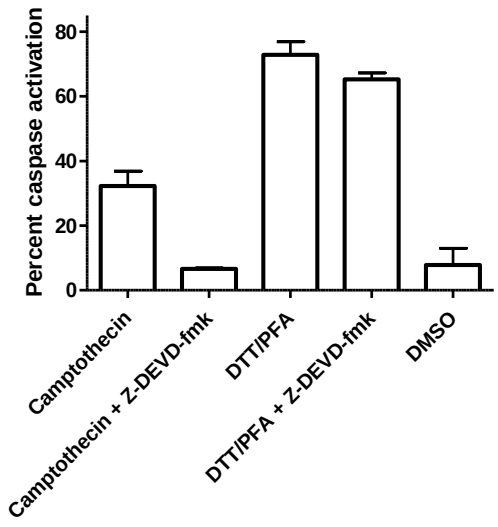

Figure 17: Z-DEVD-fmk does not inhibit caspase-3 during GPMV formation. Cells were treated with 10μM camptothecin as a positive control to induce apoptosis or with GPMV buffer for 45min at 37C followed by labeling with a caspase 3/7 detection reagent. Cells were pre-treated with Z-DEVD-fmk, which was present in all buffers throughout each experiment. Z-DEVD-fmk was successful in inhibiting caspase-3 activation in CPT treated cells. However, it was unable to prevent caspase-3 activation during GPMV formation with DTT/PFA.

Aim 2: Measuring the effect of PS asymmetry on mast cell activation (degranulation).

The next aim of this project was to determine the effect of PS asymmetry and its transient loss on immune cell signaling, specifically on mast cell activation and degranulation. Here, we will evaluate the functional role of PS asymmetry during this process of degranulation. Mast cell activation involves the binding of antigen to FcεRI receptors on the mast cell surface, activating a variety of signaling pathways that result in PKC activation and mobilization of intracellular calcium. These steps ultimately lead to the exocytosis of histamine containing granules (Fig 2). Another consequence of the mobilization of intracellular calcium is activation of Ano6, resulting in the externalization of PS (Oh and Jung, 2016). We hypothesized that this PS externalization may be an important component of cell signaling, and therefore that inhibition of PS scrambling during antigen-mediated signaling would affect mast cell activation and secretion efficiency. To test this, RBL cells (a leukemic mast cell line) were activated in the presence of the Ca^{2+}-activated chloride channel / scramblase inhibitor A01. Secretion efficiency was determined by measuring beta-hexaminidase (which resides in histamine granules) in the secreted medium relative to the same enzyme (beta-hex) remaining in the cells. As a positive control, PMA and ionomycin were used to bypass the antigen mediated steps in this pathway, by increasing PKC activation and calcium levels directly. Fig18 shows that the scramblase inhibitor A01 abrogates antigen mediated secretion in mast cells. Basal levels of

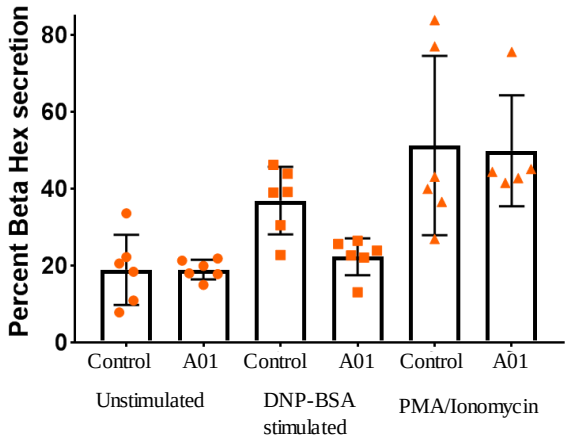

Figure 18: Scramblase inhibitor (A01) abrogates antigen mediated secretion. Stimulation with antigen increases granule exocytosis (estimated from beta-hexaminidase secretion to ~40% from 20% in unstimulated cells. Treatment of cells with A01 (a scramblase inhibitor) completely abrogated antigen-mediated secretion with no effect on basal secretion or secretion induced by PMA and ionomycin, which bypass antigen mediated signaling to directly activate secretion. This finding indicates that PS externalization (via Ano6) is required for pathways upstream from PKC in order to mediate degranulation.

secretion for both A01 treated and untreated cells was ~20%. Stimulation with antigen increased secretion to ~40%, whereas antigen stimulation in the presence of A01 resulted in no increase in secretion compared to basal. These results suggest that A01 is capable of abrogating antigen mediated stimulation, possibly through inhibition of Ano6 activation and PS externalization. The control results suggest that PS scrambling is necessary for activation of PKC and other upstream pathways, and that secretion is not affected when antigen mediated simulation is bypassed. However, it will be important to verify that A01 is preventing the externalization of PS.

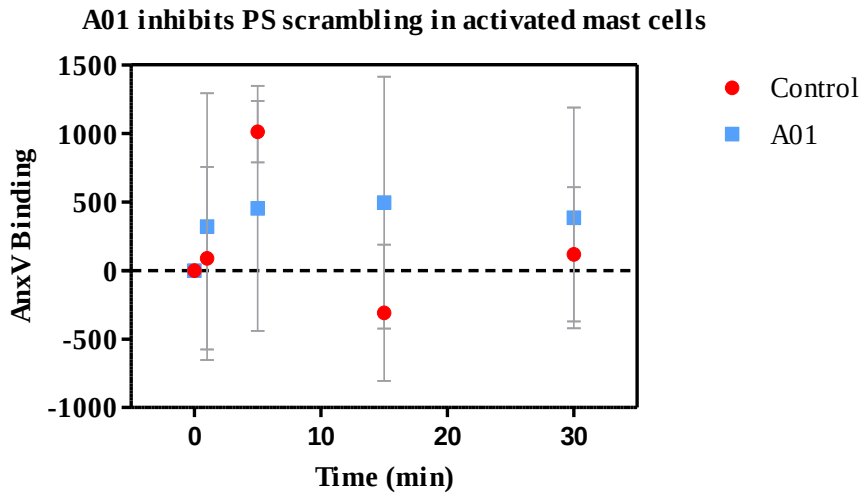

Figure 19: A01 inhibits PS scrambling in activated mast cells: Measurement of PS externalization (measured by AnxV binding) in mast cells (RBL) upon antigen mediated activation and degranulation. After 5min, PS externalization appears to maximize in the control group. Over the course of the next 10 minutes, PS begins to re-internalize, as measured by a decrease in AnxV binding from 5 to 15min. When cells are treated with A01 prior to and during antigen mediated stimulation, we see a very small increase in externalized PS, but not to the same levels as observed in the untreated control groups, and is not followed by any marked decrease in externalized PS up to 30min.

PS externalization during degranulation is inhibited by A01.

To verify that A01 was preventing externalization of PS during RBL activation and degranulation, cells were activated for varying times (1, 5, 10, 15 and 30 min) in the presence or absence of A01 and external PS was labeled with AnxV after fixing. AnxV binding was measured using a Tecan plate reader. Figure 19 shows that A01 does inhibit PS externalization in activated mast cells. This data lends credence to the possibility that PS externalization is required for antigen mediated mast cell activation, and inhibition using A01 results in an overall decrease in secretion efficiency of beta-hex.

Charge-based interaction of proteins with the electronegative inner leaflet of the PM.

Our previous results suggest calcium-mediated PS scrambling may be an important component of mast cell signaling and activation. To explain the potential mechanism by which this effect might be occurring, we hypothesized that scrambling of PS changes the electrostatic charge of the inner leaflet of the PM, regulating protein localization. We investigated this hypothesis by investigating the effects of PS scrambling on the localization of LactC2 (the PS binding fragment of the lacthedrin protein) and K-Ras(Lee et al., 2012; Zhou et al., 2014, 2015, 2017), which has been shown to have a strong interaction with the negatively charged inner leaflet of the plasma membrane(Gelabert-Baldrich et al., 2014) (Fig 20). WT or Ano6 KO HeLa cells were transfected with either GFP labeled LactC2 or K-Ras and subjected to ionomycin-mediated calcium stimulation to induce PS scrambling. In WT cells, ionomycin resulted in the relocalization of both LactC2 and K-Ras from the PM to intracellular compartments, including the Golgi and ER, as identified by the morphology of the staining. In Ano6 KOs, both LactC2 and K-Ras remain largely PM bound following ionomycin stimulation (Fig 21-22). Binding of LactC2 and K-Ras to the PM was quantified by comparing the fluorescence intensity of the PM of transfected cells to the intracellular fluorescence using images captured before and during ionomycin mediated Ca^{2+} stimulation (Fig 23). In both control groups, PM bound LactC2 and K-Ras are rapidly re-localized during ionomycin mediated Ca^{2+} stimulation. However, in both Ano6 KO groups, the overall trend

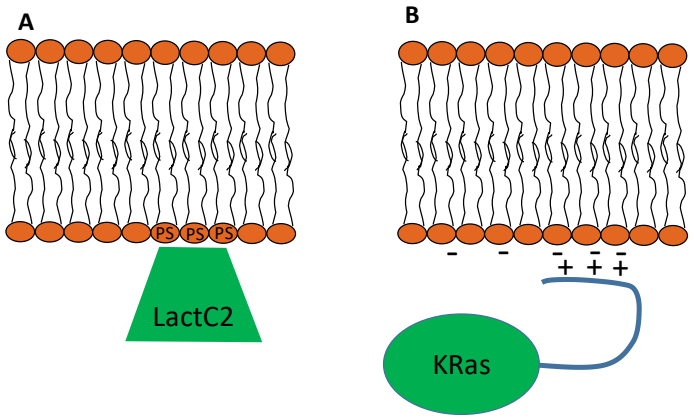

Figure 20: Representation of interaction of LactC2 and K-Ras with the negatively charged PS in the plasma membrane. A) LactC2 is a section of the lactadherin protein that specifically binds to PS in the plasma membrane. **B)** K-Ras contains a post translational modification that allows for binding to the negatively charged lipids within the inner leaflet of the plasma membrane

indicates that LactC2 and K-Ras remain mostly PM bound during ionomycin mediated Ca^{2+} stimulation. These results suggest that relocalization of LactC2 and K-Ras during ionomycin mediated calcium stimulation is due to the change of the electronegative inner leaflet of the PM and / or a decrease in the concentration of inner leaflet PS. As the concentration of internal PS decreases, LactC2 and K-Ras may be mislocalizing from an area of low PS concentration (cytosolic PM leaflet), to an area of higher PS concentration (i.e. Golgi and ER). These results also suggest a mechanism by which certain cellular pathways may be regulated by PS scrambling. This relocalization may be important in functioning as a negative regulator of various signaling pathways within cells, specifically those involving Ca^{2+} signaling. For example, K-Ras that is PM bound is typically in its active form(van der Hoeven et al., 2013; Schmick et al., 2014). One of the consequences of active K-Ras signaling is the mobilization of intracellular calcium(Fujimoto et al., 2011). This mobilization of intracellular Ca^{2+} may result in the activation of Ano6, scrambling of PS, and the relocalization of K-Ras, shutting down the pathway. More research will be needed to determine if the activity of this pathway is affected by the loss of PS asymmetry.

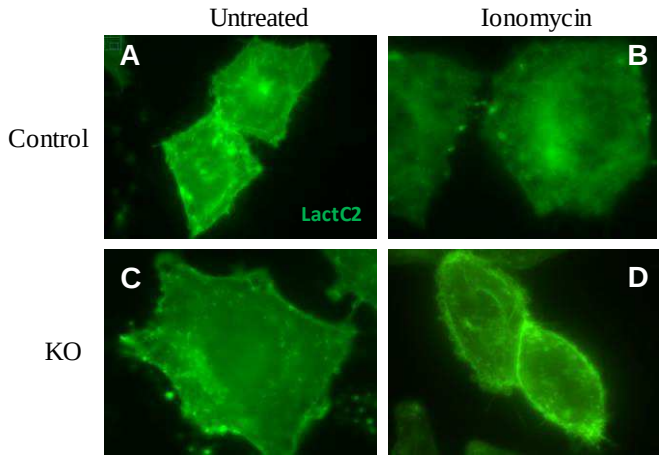

Figure 21: Relocalization of LactC2 in HeLa cells during ionomycin mediated calcium stimulation. **A)** Cells transfected with plasmids for GFP labeled LactC2 show this protein preferentially localizing to the plasma membrane of the cells **B)** During inomycin mediated calcium stimulation of WT HeLa cells, LactC2 is shown to relocalize from the membrane to intracellular components such as the Golgi and ER. **C)** As in WT cells, LactC2 is preferentially localized to the PM in Ano6 KO resting cells but **D)** during ionomcyin mediated calcium stimulation, PS is not scrambled and LactC2 remains mostly bound to the plasma membrane

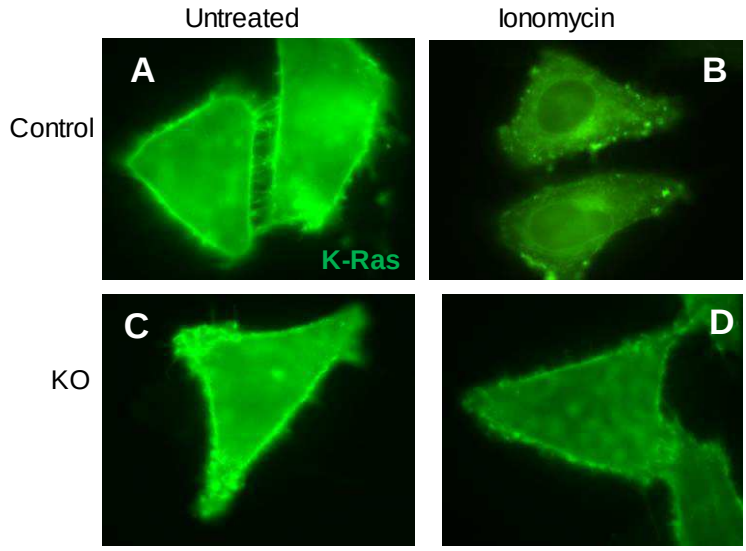

Figure 22: Mislocalization of K-Ras in HeLa cells during ionomycin mediated calcium stimulation. **A)** Cells transfected with plasmids for GFP labeled K-Ras show this protein preferentially localizing to the plasma membrane of the cells **B)** During inomycin mediated calcium stimulation of WT HeLa cells, K-Ras is shown to mislocalize from the membrane to intracellular components such as the Golgi and ER. **C)** As in WT cells, K-Ras is preferentially localized to the PM in Ano6 KO resting cells but **D)** during ionomcyin mediated calcium stimulation, PS is not scrambled and K-Ras remains mostly bound to the plasma membrane

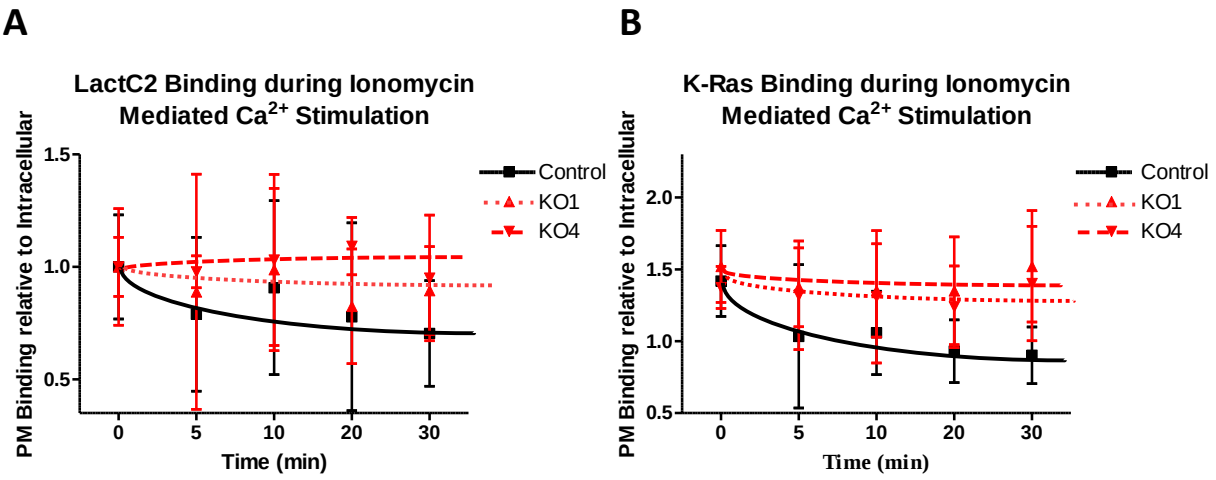

Figure 23: K-Ras and LactC2 remain PM bound in Ano6 KO HeLa during Ca^{2+} stimulation. A) In both Ano6 KO clones (inhibition of PS scrambling), PM binding of LactC2 remains mostly unchanged during ionomycin mediated Ca^{2+} stimulation, whereas LactC2 relocalization in control cells occurs rapidly (within 5 min following stimulation). This effect is more prominent in cells expressing with K-Ras **(B)** which is not re-localized and remains mostly PM bound in both Ano6 KO clones compared to control cells.

DISCUSSION

To study the biophysical properties of the plasma membrane (PM), we utilize a method which involves the chemical isolation of PM vesicles (known as Giant Plasma Membrane Vesicles; GPMVs) induced by NEM or PFA/DTT in a Ca^{2+} containing buffer. These GPMVs provide a simple model system to study the biophysical properties of the plasma membrane, including lipid distribution between leaflets, lipid packing, as well as the separation of the plasma membrane into coexisting liquid phases. Currently, this model system is the most representative system for studying the biophysical properties of the isolated plasma membrane; however, it is not fully representative of the native state of the PM in living cells. GPMVs that are produced from cells lose the native lipid leaflet asymmetry normally found in living cells. We can show this lack of strict lipid asymmetry in GPMVs by utilizing Annexin V (AnxV) as a marker for externally-exposed phosphatidylserine (PS). In live cells, PS is found almost exclusively on the inner (cytoplasmic) leaflet of the plasma membrane bilayer. In contrast, in isolated GPMVs, PS is externalized. It has been shown that GPMV inducing reagents such as DTT/PFA induce a constant Ca^{2+} influx(Keller et al., 2009). This constant Ca^{2+} flux may be responsible for the activation of the Ca^{2+} activated chloride channel scramblase Anoctamin 6 (Ano6) resulting in the externalization of PS during GPMV formation. Studies have shown that inhibition or knockdown of Ano6 results in an inability of cells to externalize PS during Ca^{2+} mediated cell signaling(Ousingsawat et al., 2015). We hypothesized that targeting of Ano6 would result in the production of cells that do not externalize PS during Ca^{2+} mediated GPMV formation. We first sought to inhibit the PS scrambling protein Ano6 through utilization of a Ca^{2+} activated Cl^- channel inhibiting drug, A01.

Chemical inhibition of scramblase produces PS asymmetric GPMVs, but abrogates phase separation.

Our initial results had shown that targeting of the Ca^{2+} activated chloride channel scramblase Ano6 in RBLs (via chemical inhibition with A01) is capable of producing PS asymmetric GPMVs. We used a Ca^{2+} activated chloride channel inhibitor, A01, to successfully inhibit the scramblase, which yielded PS asymmetric GPMVs as evidenced by a lack of AnxV568 binding (see Fig 3). We next analyzed the biophysical properties of these PS-asymmetric GPMVs, and observed a dramatic change in the appearance / stability of Lo/Ld phase separation. Specifically, phase separation was not observable in GPMVs produced with A01, even at temperatures as low as 2°C. Typical temperatures at which phase separation is first observable in GPMVs produced from RBLs are ~15°C.

Initially, this was an exciting result, as it appeared that lipid asymmetry was dramatically affecting biophysical properties of the PM bilayer, with asymmetric vesicles being unable to phase separate while PS-scrambled ones did. Unfortunately, we then noted that the addition of A01 to GPMVs *after* production (when asymmetry is already lost), at the same concentrations used for inhibition of scrambling, also lowered phase separation temperatures and led to a complete abrogation of phase separation in these GPMVs. Thus, the effect of the drug alone on isolated PMs was essentially equivalent to the effect of the drug on cells during GPMV isolation, suggesting that the observed biophysical effects were more likely the result of a non-specific interaction(s) of the drug with the membrane, rather than a specific effect of PS asymmetry.

We next attempted a number of methods to remove A01 from isolated asymmetric GPMVs and thereby remove the biophysical effects of this drug and measure any possible effects of asymmetry. To verify that A01 was being successfully removed, we used phase separation in GPMVs as a read-out: after GPMVs were isolated, A01 was added at concentrations that were

shown to completely abrogate phase separation (50μM). These GPMVs were next dialyzed for 2, 4 or 24hrs in GPMV buffer and observed to determine if phase separation had returned, which would be evidence that the drug was removed. Dialysis was shown to be unsuccessful in removing A01, as we observed no return on phase separation. We next attempted to remove A01 from GPMVs using adsorbent Bio-Beads. These Bio-Beads are designed to remove lipophilic compounds and detergents from solutions. As with dialysis, there was no observable return of phase separation to these GPMVs, and we concluded that this method was unsuccessful in removing A01. Finally, we attempted to remove A01 by utilizing small unilamellar vesicles (SUVs). We hypothesized that SUVs would add a large pool of membranes, thereby effectively diluting the drug from the GPMVs. However, like the previous attempts to remove A01, this method also proved unsuccessful, as addition of SUVs to GPMVs treated with A01 showed no return of phase separation.

Genetically targeting the Ca^{2+} activated chloride channel Ano6.

Although the Ca^{2+} activated Cl^- channel inhibitor A01 was shown to successfully inhibit PS externalization during GPMV formation in RBLs, likely through targeting of Ano6, we were unable to examine the biophysical properties of GPMVs produced with A01, because of the artefactual behavior of this drug. Since we were unable to remove this drug from GPMVs after production, we changed tracks to test whether we could produce PS-asymmetric GPMVs by genetically targeting the Ca^{2+} activated Cl^- channel scramblase Ano6. siRNA knockdown of Ano6 resulted in the production of PS asymmetric GPMVs, as shown through AnxV labeling and flow analysis of AnxV binding to GPMVs. These results suggest that eliminating the Ca^{2+} Cl^- channel scramblase Ano6 was sufficient for the production of a cell line capable of maintaining PS asymmetry during GPMV formation.

Since knockdown of Ano6 in RBLs resulted in the production of PS asymmetric GPMVs, we decided that the next step should be to produce a stable Ano6 knockout cell line, as these would presumably be more repeatable and robust, because of the absolute lack of this protein. Further, we could then use these lines for molecular/cell biology analyses of the effect of PS-asymmetry (and the loss thereof) on various signaling pathways. To produce this knockout cell line, we utilized the CRISPR/Cas9 system, which creates a double strand break at a specified target sequence on the genome, resulting in the activation of the non-homologous end joining repair pathway. We determined if these plasmids would produce a population of RBL cells which did not externalize PS during calcium mediated stimulation. Ca^{2+} stimulation was mediated using ionomycin, followed by labeling of external PS using AnxV568 and quantification by flow cytometry. Transfection of RBLs with CRISPR plasmids containing either gRNA-1 or gRNA-2 were successful in producing cells that did not externalize PS during ionomycin mediated calcium stimulation. Cells were next sorted, based on this lack of AnxV568 binding (thus no PS externalization), using fluorescence activated cell sorting (FACS). After sorting, the population of cells that did not externalize PS increased from ~20% to ~50% pre-to post sorting, respectively. We initially expected this population of cells that do not externalize PS to be 100% and not 50%. It is possible that during this sorting process, a population of WT cells which did not externalize PS during ionomycin mediated Ca^{2+} stimulation, for an unknown reason, were sorted along with our Ano6 KO cells. However, two days after the initial ionomycin mediated Ca^{2+} stimulation assay, when it was performed again, we observed a very rapid decrease in the number of cells that did not externalize PS compared to previous results. 4 days after the initial assay, the population of cells that did not externalize PS had completely disappeared. This transfecting and sorting process was repeated, with the same results. Based on these results, we hypothesized that targeting of Ano6 for knockout resulted in the production of a population of cells that was being out-competed for growth compared to WT cells due to this phenotypic change.

In order to circumvent the potential growth competition between Ano6 WT and Ano6 KO RBLs, cells were transfected and clonally selected. Single cells which expressed GFP (as an indication of successful transfection of CRISPR plasmid) were sorted (using FACS) into a 96-well dish containing conditioned RBL growth medium (equal volumes of RBL growth medium supplemented with culture medium partially used by cells). Once colonies expanded sufficiently, genomic analysis was performed on each of the recovered clones. Only six of the 96-wells successfully grew up into colonies and genomic analysis of these clones revealed that they had a WT genotype. In some wells, however, we observed single cells which did not divide after more than a month. Single cell sorting was performed 3 different times by three different experimenters, all with the same results – namely growth of only WT cells (as determined by genomic analysis). Therefore, we concluded that our protocol for producing Ano6 knockouts were leading to cell lethality, either because Ano6 is an essential gene in RBLs or because of off target effects.

Development of Ano6 KO in HeLa using CRISPR.

To overcome this limitation of Ano6 KO lethality in RBLs, we next switched to developing an Ano6 KO cell line from HeLa cells, as these cells are easier to transfect than RBLs and also from a completely different tissue source (endometrial versus hematopoietic). Single cell cloning revealed that, in contrast to RBLs, most of the HeLa wells grew into stable colonies. Genomic analysis revealed that two of the three colonies analyzed showed alterations to the target genome site: one showing a single base pair insertion and the other showing an insertion / deletion mutation. We verified that these lines were knockouts by Western blotting, which showed an absence of Ano6 in both KO clones compared to the WT. Similarly, PS externalization during ionomycin-mediated Ca^{2+} stimulation was analyzed using AnxV568, revealing a significant population of clonally selected cells which did not externalize PS during ionomycin stimulation; similar to RBLs when Ano6 was

knocked down or inhibited (see Fig3,7). Thus, we successfully produced Ano6 knockout cell lines that had the desired phenotype of failing to expose PS during Ca^{2+} stimulation.

Isolation of GPMVs from HeLa Ano6 KO Clones.

After verification that Ano6 was successfully knocked out, we produced GPMVs from both Ano6 KO cell lines (termed KO1 and KO4) to determine if they would be PS-asymmetric. Although there was a small decrease in the overall fluorescence intensity in AnxV568 binding in Ano6 KO1 and KO4 cells compared to the WT HeLa cells, these differences were not statistically significant (see Fig 14). Surprisingly, two of 10 experiments produced exactly the expected/desired results; minimal AnxV568 binding (thus no PS externalization) in KO1 and KO4 compared to robust AnxV binding to WT GPMVs. However, this effect was not repeatable and we were unable to find the source of this variation. We speculate that this variation may be due to the presence of other scramblases or Anoctamin family proteins in HeLa that are not present in RBLs.

We postulated that alternative scramblase proteins to Ano6 may be activated by the process of GPMV formation, and identified as likely candidates either (1) other Anoctamin family proteins; or (2) Xkr8, a protein shown to exhibit caspase-3 dependent scramblase activity during apoptosis(Suzuki et al., 2014). Focusing first on Xkr8, we determined whether GPMV formation resulted in the activation of caspase-3. Since Xkr8 is a caspase-3 dependent PS scramblase, activation of caspase-3 would likely result in subsequent activation of Xkr8 and scrambling of PS during GPMV formation. This would potentially explain the externalization of PS observed during GPMV formation in Ano6 KO HeLa cells and shed some light on the process by which GPMVs are formed. Our results indicated that caspase-3 was indeed being activated during GPMV formation with either NEM and DTT/PFA. It is unusual that NEM based GPMV production results in the activation of caspase-3, as NEM is very specific in targeting thiols, and is commonly used to modify

and target cysteine residues, therefore it should act as an inhibitor or caspase-3. We then hypothesized that blocking caspase-3 activity during GPMV formation may inhibit Xkr8 activation and therefore PS scrambling. We attempted to inhibit caspase-3 activity with the widely-used small molecule Z-DEVD-fmk. This drug is considered relatively selective for caspase-3 among others(Garcia-Calvo et al., 1998). Surprisingly, Z-DEVD-fmk was unable to prevent the activation of caspase-3 during GPMV formation. We are unsure why this drug was unsuccessful in preventing caspase-3 activation, especially when GPMVs are isolated with NEM. Since caspase-3 is a member of the cysteine-aspartic acid protease family, and its active site contains a cysteine residue, the presence of NEM should directly inhibit caspase-3 activation in HeLa. Thus, there should not be any interaction between NEM and Z-DEVD-fmk, as there are no cysteine residues on Z-DEVD-fmk. Currently, it is unclear why Z-DEVD-fmk is not efficiently inhibiting caspase-3 during GPMV isolation. It is worth noting here that this drug was capable of inhibiting caspase-3 activation in control conditions (camptothecin-induced apoptosis).

Future directions: targeting other scramblase proteins in HeLa to produce PS asymmetric GPMVs.

Since we were unable to prevent caspase-3 activation during GPMV formation in HeLa with a caspase-3 inhibiting drug, the next step would be to target Xkr8 directly for either knockdown or knockout. Future experiments should also focus on the targeted knockout or knockdown of other scramblases found in these cells. Specifically, Suzuki et al 2013 showed expression of two additional anoctamin scramblases, Ano4 and Ano9 in mouse ovarian and uterine tissues, and these proteins exhibit PS scrambling activity during Ca^{2+} stimulation[34]. It may be that these two proteins are compensating for the loss of Ano6, resulting in the scrambling of PS during GPMV formation. Notably, it was shown that mouse tissues involved in immunity expressed only a single PS

scrambling anoctamin, i.e. Ano6. If the same is true for RBLs, it may be postulated that the only protein responsible for scrambling of PS during Ca^{2+} mediated signaling in these cells is Ano6. This could serve to explain why siRNA targeted knockdown of Ano6 worked so well in RBLs, but knocking out Ano6 in HeLa did not work, in that other anoctamin scramblases are expressed in HeLa which are capable of compensating for the loss of Ano6, but there are no other anoctamin scramblases expressed in RBLs. This could also explain why RBL Ano6 KO clones were unable to divide, and why we observed such a large decrease in the population of Ano6 KO cells over time; Ano6 (and thus Ca^{2+} mediated scrambling) may be essential for normal cellular functions, such as cytokinesis. If this is true, then the presence of other Ca^{2+} mediated scrambling proteins (Ano4 and Ano6) in HeLa may be compensating for the loss of Ano6, resulting in viable clones, but also externalization of PS during GPMV formation. To test these hypotheses, and towards the ultimate goal of producing PS-asymmetric GPMVs, we have now developed multiplexed CRISPR plasmids to target Ano6, Ano4, Ano9 and Xkr8 in human cells. Multiplexing CRISPR plasmids involves the insertion of two independent gRNA sequences onto a single CRISPR backbone. This allows for the production of two Cas9 proteins, targeting two different regions of the target genome, resulting in two double strand breaks in the DNA and removal of multiple exons within a gene. This method will allow for more efficient screening to determine which combination of gene knockouts will be most effective in producing PS asymmetric GPMVs. The next steps will be the transfection of HeLa or HEK cells with various combinations of these plasmids, followed by qPCR to determine knock-out efficiency. Next GPMVs will be produced and asymmetry assayed as above. Once we establish a combination of gene knockouts that produce PS asymmetric GPMVs, we can begin to analyze their biophysical properties including phase separation, membrane diffusivity, etc.

Aim 2: Measuring the effect of PS asymmetry, by chemical inhibition of Ano6 on mast cell activation (degranulation).

The second aspect of this project was to determine the functional role of PS asymmetry, and its transient loss, on the activation of immune cells. To this end, we measured the effect of PS asymmetry on antigen-induced activation of mast cells. Specifically, a mast cell line (rat basophilic leukemia; RBL) can be induced to activate by treatment with IgE antibodies and their cognate, oligomeric antigens. Upon activation, these cells secrete a variety of inflammatory mediators (e.g. histamine and serotonin), but also the secretory granule enzyme beta-hexosaminidase. The activity of this enzyme can be quantified using standard protocols and gives a robust proxy for the efficiency of activation/degranulation. We compared secreted beta-hex between untreated cells, and those in which scrambling was inhibited, to determine the effect of PS-asymmetry on the degranulation process. If PS scrambling is important for mast cell activation, we expected to observe differences in the efficiency of secretion of beta-hex in cells there were unable to properly scramble PS.

Because we were unable to develop a stable Ano6 KO RBL line, we utilized A01 to prevent PS externalization during degranulation in RBLs. The degranulation process involves several steps, beginning with the binding of IgE-bound antigen to the FceRI receptor, followed by the initiation of downstream signaling, most notably the mobilization of intracellular Ca^{2+} and activation of PKC, leading to eventual granule secretion. We showed that during the degranulation process, PS is rapidly externalized on RBLs (as measured by AnxV568 binding) followed by a slower return to basal levels of external PS (Fig 19) This suggests that the Ca^{2+} fluxes present during RBL signaling also induce the activation of Ano6, resulting in the externalization of PS. When cells were stimulated to degranulate in the presence of A01, we showed that PS was not externalized during the degranulation process, as expected if we effectively inhibited PS scrambling activity (presumably of

Ano6). Remarkably, this inhibition of PS externalization during degranulation resulted in a decrease in the secretion efficiency of beta-hex. Notably, we also observed that secretion mediated by our positive control, i.e. treatment with ionomycin and PMA, was not affected by A01. PMA and ionomycin activate PKC and increase intracellular Ca^{2+} respectively, bypassing the antigen binding step. These results indicate that PS scrambling may be important in the initial steps of degranulation, and that preventing this PS scrambling may thus inhibit other downstream signaling effects. This could indicate a mechanism by which certain pathways within the cell are regulated by PS externalization. For example, this degranulation process may be negatively regulated by increases of intracellular Ca^{2+}. Once intracellular Ca^{2+} reaches a high enough concentration for a long enough period of time (as a consequence of the mobilization of Ca^{2+} during degranulation), PS may be scrambled via Ano6, leading to a re-localization of membrane bound proteins, ultimately "turning off" the degranulation pathway. This potential regulatory mechanism may be utilized by multiple pathways involving intracellular Ca^{2+} signaling, serving as an "off switch" for a variety of pathways.

Effect of PS scrambling on charged proteins which interact with the electronegative inner leaflet of the PM.

To elucidate the mechanism by which inhibiting PS scrambling could affect cell signaling, we used the HeLa Ano6 KO cell lines, transfecting them with plasmids coding for GFP labeled LactC2 and K-Ras(Lee et al., 2012; Zhou et al., 2014, 2015, 2017). We hypothesized that ionomycin-mediated Ca^{2+} stimulation would lead to scrambling of PS via Ano6 in WT cells, resulting in a re-localization of both LactC2 and K-Ras, whereas in Ano6 KOs we would not observe this re-localization. LactC2 is the PS binding portion of the lactahedrin protein, while the C-terminal region of K-Ras interacts with the strong electronegative charge of the inner leaflet of the PM. Both of these proteins are located primarily at the inner leaflet of the plasma membrane in unstimulated

cells. When PS scrambling was induced through ionomycin mediated Ca^{2+} stimulation in WT HeLa, both LactC2 and K-Ras re-localized from the PM to intracellular compartments of the cell (Fig 21-22), including the Golgi and ER as identified by the morphology of the staining. We hypothesize that this re-localization is occurring due to the externalization of PS during Ca^{2+} flux, resulting in a change in the electronegative inner leaflet, and decrease in the concentration of PS, causing both LactC2 and K-Ras to translocate from an area of lower PS concentration (scrambled PM) to areas containing higher concentration of PS (cytoplasmic leaflets of other organelles). This inference is supported by the observations that when Ano6 KO cells were subjected to ionomycin mediated Ca^{2+} stimulation, both LactC2 and K-Ras remained largely PM bound. Thus, failure to scramble PS inhibits relocalization of a PS sensor (LactC2) and a charge sensor (K-Ras) from the PM during cell activation. These results may indicate a mechanism whereby certain cellular pathways are regulated by PS scrambling. Since active K-Ras interacts with its upstream regulators and downstream effectors at the PM, is it possible that increases in intracellular Ca^{2+} downstream of immune receptor engagement result in the activation of Ano6 (and/or other scramblase proteins), causing externalization of PS and leading to re-localization and deactivation of K-Ras. Future experiments to determine this will include comparing K-Ras signaling in Ano6 KOs compared to WT cells.

MATERIALS and METHODS

Cell culture.

RBL cells were cultured in medium containing 60% MEM, 30% RPMI medium, 10% FBS, 2mM glutamine, 100units/mL penicillin and 100µg/mL streptomycin at 37°C in humidified 5% CO_2. HeLa cells were cultured in medium containing 90% EMEM, 10% FBS, 2mM glutamine, 100units/mL penicillin and 100µg/mL streptomycin at 37°C in humidified 5% CO_2.

GPMV Isolation, Labeling, Treatment and Analysis.

GPMVs were isolated and imaged under temperature controlled conditions(Sezgin et al., 2012). For post-isolation treatments, isolation chemicals were removed by dialysis in GPMV buffer (150mM NaCl, 2mM $CaCl_2$, 10mM HEPES pH 7.4). For GPMVs dialyzed with Bio-Beads (Bio-Rad), GPMVs were placed in dialysis tubing (ThermoFishser 10K molecular weight cutoff) and placed in a solution of GPMV buffer containing 0.1g/mL Bio-Beads and left at 4°C for 2, 4 or 24hrs prior to analysis. In order to produce PS asymmetric GPMVs through chemical inhibition of Ano6, using a calcium activated chloride channel inhibitor, A01 (6-(1,1-Dimethylethyl)-2-[(2-furanylcarbonyl)amino]-4,5,6,7-tetrahydrobenzo[*b*]thiophene-3-carboxylic acid: CalBiochem) was added to GPMV buffer at a concentration of 150µM.

Analysis of AnxV Binding to GPMVs.

External PS was labeled using AnxV Alexa Fluor 568 (AnxV568) on GPMVs during the production process. Stock solutions of AnxV568 (ThermoFisher catalog: A13202) were diluted 1:100 in GPMV buffer prior to addition to cells to produce GPMVs. GPMVs were labeled with Fast DiO (ThermoFisher), a nonspecific membrane binding green fluorescent dye. This dye was used as a positive control to confirm that GPMVs were successfully produced. After production, GPMVs were

collected and imaged using fluorescence microscopy. Vesicles were first visualized via Fast DiO staining, then the same vesicles were imaged for AnxV568 binding. Images were analyzed in ImageJ: a line was drawn through each GPMV labeled with Fast DiO. Then an intensity scan was made in the AnxV568 channel, with the fluorescence intensity of each vesicle compared to that of the background in each image. Data was represented as the fold intensity of AnxV568 fluorescence to background.

Ano6 siRNA Knockdown and Analysis of Ano6 in RBLs.

Silencer Select® siRNA targeting rat Ano6 was purchased from ThermoFisher (catalog number 4390771, Assay ID: s163856, s163857, s163858). Three sequences were available and purchased. For transfection, RBLs were trypsinized, resuspended in RBL culture medium, and centrifuged at 300xg for 5min. Medium was removed, and ~1e6 cells resuspended in 100uL Mirus Buffer containing 15uL of either siRNA 1, 2, 3 or a mixture (5uL of each sequence). Cells were transfected with siRNA by electroporation at 960 Ohms and 320V for ~14msec. After 48-72hrs of recovery, GPMVs were produced from cells and external PS was labeled as above. Flow cytometry (BD LSR Fortessa Cell Analyzer System) was used to analyze AnxV568 binding to external PS in GPMVs. Unlabeled GPMVs were used to set the threshold for AnxV-negative vesicles, while GPMVs produced from WT cells (labeled with AnxV568) were used to define the maximum for AnxV568 binding.

Development of CRISPR/Cas9 Plasmids.

Plasmids were obtained from Addgene. Empty CRISPR/Cas9 plasmid was purchased from Addgene. The plasmid used was designated pSpCas9(BB)-2A-GFP (PX458) and contains a single

cloning backbone for sgRNA and a GFP reporter gene. The target sequences (see below) were cloned into the empty backbone using the Zhang Lab protocol(Ran et al., 2013). The sense sequence of the gRNA contained the 5'CACCGNNNNNNNNNNNNNNNNNN3' format (oligo 1), while the antisense sequence contained the 5'CNNNNNNNNNNNNNNNNNNNCAAA3' format (oligo 2). Oligos were annealed in the following manner: 1µL of oligo 1 (100µM), 1µL oligo 2 (100µM), 1uL 10X T4 ligation Buffer (NEB), 6.5µL ddH_2O, 0.5µL T4 PNK (NEB) final volume 10uL. Oligos were annealed in a thermocycler (Bio-Rad) using the following parameters: 37°C 30 min, 95°C 5 min, then ramp down to 25°C at 5°C/min. The annealed strand was ligated into the empty backbone using T4 DNA ligase with protocol provided by manufacturer. For ligation, using a thermocycler: 37°C 5min, 25°C 5min, repeat 6-12 times. *E. coli* DH5α cells were transformed with this digested/ligated product in the following manner: Thaw cells on ice 30min, add 2µL digested/ligated product to 50µL cells and place back on ice 10min. Remove from ice, incubate at 42°C for 60sec. Add 450µL pre-warmed SOC medium to bacteria/DNA and incubate at 37°C, 300RPM for 1hr. Add 100uL bacteria to an LB agar plate (100µM Ampicillin) and spread. Incubate at 37°C overnight. The next day, pick colonies from dish, and grow in LB medium containing 100µM ampicillin overnight at 37°C, 250RPM. Isolate plasmids using the Qiagen mini-prep plasmid isolation kit following established instructions.

CRISPR/Cas9 gRNA Plasmids, Transfection and Clonal Selection in RBLs

For Ano6 KO in RBLs

gRNA sequence 1: CACCGACTCGCTCTTTTTCACCGATGG

gRNA sequence 2: CACCGTACGAAGACGAGAGCAAGAAGG

Both sequences were designed to target exon 2 in the Ano6 gene. RBLs were transfected in the same manner as above (siRNA knockdown). 2ug of CRISPR/Cas9 plasmid were used for transfection.

24hrs after transfection, cells were sorted by MD Anderson Flow Cytometry Core and selected for GFP expression. For genomic analysis of the region targeted by gRNA 1 or gRNA2, genomic DNA was isolated using the NucleoSpin® Tissue Kit (Macherey-Nagel) following manufacturer's protocol. After isolation, PCR amplification was performed on the genomic region targeted by the CRISPR/Cas9 plasmid.

PCR forward primer: TCCTGCACAAGCATTCTAGGCTACT

PCR reverse primer: TGCTCTGCACATACAAAGTGTAATCCC

After amplification, the PCR product was sequenced by GeneWiz using the PCR forward and PCR reverse primers listed above.

Bulk Sorting of CRISPR/Cas9 Transfected (Ano6 KO) RBLs.

48hrs after transfection of RBLs with CRISPR/Cas9 targeting Ano6, cells were sorted based on lack of AnxV568 binding using Flow Activated Cell Sorting (FACS) at the MD Anderson Flow Cytometry Core. Cells were incubated with 5μM ionomycin in Tyrode's buffer (containing a 1:100 diluted AnxV568) at 37°C for 5min. Cells were then FACS-sorted, keeping only cells that did not bind AnxV568 (thresholds for binding set as above). These sorted cells were cultured for at least 7 days to allow recovery after sorting prior to further analysis.

Flow Cytometry Analysis of Ano6 KO RBLs.

RBL cells were trypsinized, resuspended in RBL culture medium, and centrifuged. After this, medium was removed and cells resuspended in Tyrode's Buffer (135mM NaCl, 5mM KCl, 1.8mM $CaCl_2$, 1mM $MgCl_2$, 5.6mM glucose, 20mM HEPES pH 7.4). PS externalization was measured using flow cytometry to monitor the extent of binding of AnxV568 to external PS in intact live cells

(BD LSR Fortessa Cell Analyzer Systems). PS externalization was mediated by addition of ionomycin (Sigma Aldrich, 5μM final concentration) and incubation at 37°C for 5min.

CRISPR/Cas9 gRNA Plasmids, Transfection and Clonal Selection in HeLa's.

For Ano6 KO in HeLa's, the gRNA sequence used was obtained from Horizon Discovery. gRNA sequence: TGTAAAAGTACACGCACCAT. HeLa cells were transfected with 2μg PX458 plasmid containing aforementioned gRNA sequence (as a control, unmodified PX458 plasmid) using Lipofectamine® 3000 (ThermoFisher) following the manufacturer's protocol with the following modification: cells were trypsinized, and resuspended in culture medium. Next, medium was removed, and cells re-suspended in a mixture of Lipofectamine® 3000 and DNA for 2min at room temperature. After this incubation, cells were placed on to multi-well plates containing culture medium. 24hrs after transfection, ~95% of all remaining cells were GFP+. For clonal selection, cells were counted and diluted to ½ cell per 100μL medium and placed onto a 96-well dish. After 1-week, wells that contained a single colony were selected for further expansion. Once these colonies had grown sufficiently, genomic DNA was isolated using the NucleoSpin® Tissue Kit (Macherey-Nagel). After isolation, PCR amplification was performed on the genomic region targeted by the CRISPR/Cas9 plasmid. Primer sequences used were obtained from Horizon Discovery. PCR forward primer: ATCTTCACTTTTAGTGGTGGTCTCT

PCR reverse primer: GGTAAACCAGTTGAGTGTACCAAAG

After amplification, PCR product was sequenced (Gene-Wiz) using the forward primer for sequencing.

Western Blot of Ano6.

Anti-Ano6 polyclonal antibody (N-terminus probing region: PA5-35240) was purchased from ThermoFisher. Cells were grown to confluency in a 6-well dish. Cells were washed on ice (with ice-cold PBS) 2x, followed by lysis in 100µL RIPA buffer (150mM NaCl, 1% Triton X-100, 0.1% SDS, 0.5% sodium deoxycholate, 50mM Tris pH 8.0) containing fresh DTT (100uM) and 1x proteinase inhibitor cocktail (PIC). Cells were homogenized with a 24G needle 15x and kept on ice 20min, followed by centrifugation at 12,000RPM at 4°C for 15min. Protein concentration was measured using BCA kit (Thermo Scientific). 50µg cell extract was loaded onto an 8% SDS gel and run at 80V until the dye reached the bottom of the separating gel. Transfer to PVDF membrane at 125mA, 90min with 2x transfer buffer containing 0.05% SDS. Block membrane 1hr room temperature (RT) in 5% non-fat milk (NFM) dissolved in Tris-Buffered Saline with 0.1% Tween-20 TBST. Probe overnight at 4°C with anti-Ano6 antibody (1:500 dilution from stock) in 1% NFM and TBST. Wash membrane 3 times for 10 minutes in TBST. Probe with anti-rabbit HRP antibody (SIGMA Genosys) in 3% NFM and TBST 2hrs RT. Wash membrane 3 times for 10min in TBST. Incubate in ECL solution (Bio-Rad) 10min RT and image using ChemiDoc (Bio-Rad).

Detection of Caspase-3/7.

To detect caspase-3/7 activation, HeLa cells were grown to confluency in a 96-well dish, followed by treatment with either 10µM camptothecin (Cayman Chemical Company) as a positive control (8hrs 37C in HeLa culture medium) to induce caspase3/7 activation or GPMV buffer containing 2mM NEM or 2mM DTT/25mM PFA for 45min at 37°C (to mimic conditions for GPMV production). After appropriate incubation times, cells were washed 2x with 1X PBS. Active caspase-3/7 was detected using CellEvent™ Caspase-3/7 Green Detection Reagent (ThermoFisher catalog: C10723); reagent was diluted to 7.5µM in 1X PBS containing 5% FBS at 37°C for at least 30min.

After this incubation time, cells were imaged with bright-field overlaid with GFP (bright green nuclei were considered to have active caspase-3/7). Caspase activation was calculated as a percent of cells with GFP labeled nuclei relative to the total number of cells.

Inhibition of Caspase-3/7 Activation.

Caspase-3/7 activation was inhibited using Z-DEVD-fmk purchased from Cayman Chemical Company. A 100mM stock solution in DMSO was prepared from powder. Cells were pre-treated for 1hr at 37°C in HeLa culture medium with Z-DEVD-fmk (100µM). After this pre-treatment, cells were treated with either camptothecin (10µM 8hrs 37°C) in culture medium containing 100µM Z-DEVD-fmk or GPMV buffer containing 2mM NEM or 2mM DTT/25mM PFA 45min 37°C. After this treatment, active caspase-3/7 was detected as above.

Degranulation of RBLs.

RBLs were plated such that they were 60-80% confluent in a 12-well dish the day the degranulation assay is to be performed. Cells were kept in serum free RBL culture medium overnight. Cells were sensitized for 1hr 37°C with 1.0µg/mL anit-dinitrophenol (DNP) IgE in complete RBL culture medium. Excess IgE was removed before stimulation by washing cells 3x with 1X PBS and once with Tyrode's buffer containing 1mg/mL BSA. To stimulate, 1µg/mL DNP-BSA (dinitrophenol-bovine serum albumin) was added and the cells were incubated at 37°C for 30min.

Percent secretion is measured by determining the percent of beta-hexaminidase(beta-hex) secreted as follows. Following incubation, the supernatant was removed from the cells and saved for further analysis. The cells were then lysed cells with 1% Triton X-100 (volume equivalent to buffer volume used during stimulation) for 5min at 37°C. This lysate and the supernatant above were then used to

measure the beta-hex levels in remaining and secreted fractions, respectively. To measure beta-hex, 20µL of sample (either lysate or supernatant) was combined with 80µL of 0.375mM 4-methylumbelliferyl N-acetyl-beta-D-glucosamine (dissolved in citrate buffer: 49.5mL of 0.05M citric acid and 50.5mL of 0.05M tri-sodium citrate pH 4.5) for 1hr at 37°C. The reaction was quenched by addition of 200µL of 0.05M sodium carbonate buffer (60mL of 0.05M Na_2CO_3 and 40mL of 0.05M $NaHCO_3$). The fluorescence was read using Tecan plate reader: Excitation 362, emission 448. Data was presented as percent beta-hex secreted after averaging a triplicate from each well. For cells treated with A01, drug was added to stimulation buffer to a final concentration of 150µM.

Detection of External PS on Activated RBLs.

RBLs were activated (as described above) for various time points: 1, 5, 15 and 30min. After appropriate incubation times, cells were fixed with 4% PFA for 5min on ice, followed by incubation at room temperature for 25min. Quench reaction with 100mM glycine 2x15min at RT. 1:100 dilution (in Tyrode's buffer) of AnxV568 (ThermoFisher catalog: A13202) was added to each well and incubated for 5min at RT. Fluorescence intensity was obtained using the Tecan plate reader. The average fluorescence intensity for each well was used for final analysis, normalizing to the fluorescence intensity of the unstimulated cells.

REFERENCES

Barsumian, E.L., Isersky, C., Petrino, M.G., and Siraganian, R.P. (1981). IgE-induced histamine release from rat basophilic leukemia cell lines: isolation of releasing and nonreleasing clones. Eur. J. Immunol. *11*, 317–323.

Bevers, E.M., and Williamson, P.L. (2010). Phospholipid scramblase: An update. FEBS Lett. *584*, 2724–2730.

Burns, M., Wisser, K., Wu, J., Levental, I., and Veatch, S.L. (2017). Miscibility Transition Temperature Scales with Growth Temperature in a Zebrafish Cell Line. Biophys. J.

Devaux, P.F. (1988). Phospholipid flippases. FEBS Lett. *234*, 8–12.

Fujimoto, T., Machida, T., Tsunoda, T., Doi, K., Ota, T., Kuroki, M., and Shirasawa, S. (2011). KRAS-induced actin-interacting protein regulates inositol 1,4,5-trisphosphate-receptor-mediated calcium release. Biochem. Biophys. Res. Commun. *408*, 214–217.

Galli, S.J., Starkl, P., Marichal, T., and Tsai, M. (2016). Mast cells and IgE in defense against venoms: Possible "good side" of allergy? Allergol. Int. *65*, 3–15.

Garcia-Calvo, M., Peterson, E.P., Leiting, B., Ruel, R., Nicholson, D.W., and Thornberry, N.A. (1998). Inhibition of human caspases by peptide-based and macromolecular inhibitors. J. Biol. Chem. *273*, 32608–32613.

Gelabert-Baldrich, M., Soriano-Castell, D., Calvo, M., Lu, A., Vina-Vilaseca, A., Rentero, C., Pol, A., Grinstein, S., Enrich, C., and Tebar, F. (2014). Dynamics of KRas on endosomes: involvement of acidic phospholipids in its association. FASEB J. *28*, 3023–3037.

Gyobu, S., Miyata, H., Ikawa, M., Yamazaki, D., Takeshima, H., Suzuki, J., and Nagata, S. (2016). A Role of TMEM16E Carrying a Scrambling Domain in Sperm Motility. Mol. Cell. Biol. *36*, 645–659.

van der Hoeven, D., Cho, K. -j., Ma, X., Chigurupati, S., Parton, R.G., and Hancock, J.F. (2013). Fendiline Inhibits K-Ras Plasma Membrane Localization and Blocks K-Ras Signal Transmission. Mol. Cell. Biol. *33*, 237–251.

Holowka, D., Wilkes, M., Stefan, C., and Baird, B. (2016). Roles for Ca^{2+} mobilization and its regulation in mast cell functions: recent progress. Biochem. Soc. Trans. *44*, 505–509.

Keller, H., Lorizate, M., and Schwille, P. (2009). PI(4,5)P2 Degradation Promotes the Formation of Cytoskeleton-Free Model Membrane Systems. ChemPhysChem *10*, 2805–2812.

Lee, S., Uchida, Y., Emoto, K., Umeda, M., Kuge, O., Taguchi, T., and Arai, H. (2012). Impaired retrograde membrane traffic through endosomes in a mutant CHO cell defective in phosphatidylserine synthesis. Genes Cells *17*, 728–736.

Levental, K.R., and Levental, I. (2015). Isolation of Giant Plasma Membrane Vesicles for Evaluation of Plasma Membrane Structure and Protein Partitioning. In Methods in Membrane Lipids, D.M. Owen, ed. (New York, NY: Springer New York), pp. 65–77.

Marshall, J.S. (2004). Mast-cell responses to pathogens. Nat. Rev. Immunol. *4*, 787–799.

Martin, S., Pombo, I., Poncet, P., David, B., Arock, M., and Blank, U. (2000). Immunologic stimulation of mast cells leads to the reversible exposure of phosphatidylserine in the absence of apoptosis. Int. Arch. Allergy Immunol. *123*, 249–258.

Martins, J.R., Faria, D., Kongsuphol, P., Reisch, B., Schreiber, R., and Kunzelmann, K. (2011). Anoctamin 6 is an essential component of the outwardly rectifying chloride channel. Proc. Natl. Acad. Sci. *108*, 18168–18172.

Nagata, S., Suzuki, J., Segawa, K., and Fujii, T. (2016). Exposure of phosphatidylserine on the cell surface. Cell Death Differ. *23*, 952–961.

Oh, U., and Jung, J. (2016). Cellular functions of TMEM16/anoctamin. Pflüg. Arch. - Eur. J. Physiol. *468*, 443–453.

Ousingsawat, J., Wanitchakool, P., Kmit, A., Romao, A.M., Jantarajit, W., Schreiber, R., and Kunzelmann, K. (2015). Anoctamin 6 mediates effects essential for innate immunity downstream of P2X7 receptors in macrophages. Nat. Commun. *6*, 6245.

Ran, F.A., Hsu, P.D., Wright, J., Agarwala, V., Scott, D.A., and Zhang, F. (2013). Genome engineering using the CRISPR-Cas9 system. Nat. Protoc. *8*, 2281–2308.

Ravichandran, K.S. (2010). Find-me and eat-me signals in apoptotic cell clearance: progress and conundrums. J. Exp. Med. *207*, 1807–1817.

Rosing, J., Tans, G., Govers-Riemslag, J.W., Zwaal, R.F., and Hemker, H.C. (1980). The role of phospholipids and factor Va in the prothrombinase complex. J. Biol. Chem. *255*, 274–283.

Rosing, J., Bevers, E.M., Comfurius, P., Hemker, H.C., Van Dieijen, G, Weiss, H., and Zwaal, R.F. (1985). Impaired Factor X and Prothrombin Activation Associated with Decreased Phospholipid Exposure in Platelets from a Patient with a Bleeding Disorder. Blood *11*, 380–383.

Schmick, M., Vartak, N., Papke, B., Kovacevic, M., Truxius, D.C., Rossmannek, L., and Bastiaens, P.I.H. (2014). KRas Localizes to the Plasma Membrane by Spatial Cycles of Solubilization, Trapping and Vesicular Transport. Cell *157*, 459–471.

Segawa, K., Suzuki, J., and Nagata, S. (2011). Constitutive exposure of phosphatidylserine on viable cells. Proc. Natl. Acad. Sci. *108*, 19246–19251.

Sengupta, P., Hammond, A., Holowka, D., and Baird, B. (2008). Structural determinants for partitioning of lipids and proteins between coexisting fluid phases in giant plasma membrane vesicles. Biochim. Biophys. Acta BBA - Biomembr. *1778*, 20–32.

Sezgin, E., Kaiser, H.-J., Baumgart, T., Schwille, P., Simons, K., and Levental, I. (2012). Elucidating membrane structure and protein behavior using giant plasma membrane vesicles. Nat. Protoc. *7*, 1042–1051.

Shor, E., Wang, Y., Perlin, D., and Xue, C. (2016). Cryptococcus flips its lid - membrane phospholipid asymmetry modulates antifungal drug resistance and virulence. Microb. Cell *3*, 358–360.

Simons, K., and Toomre, D. (2000). Lipid rafts and signal transduction. Nat. Rev. Mol. Cell Biol. *1*, 31.

Singh, J., Shah, R., and Singh, D. (2016). Targeting mast cells: Uncovering prolific therapeutic role in myriad diseases. Int. Immunopharmacol. *40*, 362–384.

Smrž, D., Dráberová, L. 'ubica, and Dráber, P. (2007). Non-apoptotic Phosphatidylserine Externalization Induced by Engagement of Glycosylphosphatidylinositol-anchored Proteins. J. Biol. Chem. *282*, 10487–10497.

Spronk, H.M.H., ten Cate, H., and van der Meijden, P.E.J. (2014). Differential roles of Tissue Factor and Phosphatidylserine in activation of coagulation. Thromb. Res. *133*, S54–S56.

Suzuki, J., Fujii, T., Imao, T., Ishihara, K., Kuba, H., and Nagata, S. (2013). Calcium-dependent Phospholipid Scramblase Activity of TMEM16 Protein Family Members. J. Biol. Chem. *288*, 13305–13316.

Suzuki, J., Imanishi, E., and Nagata, S. (2014). Exposure of Phosphatidylserine by Xk-related Protein Family Members during Apoptosis. J. Biol. Chem. *289*, 30257–30267.

Theoharides, T.C., Alysandratos, K.-D., Angelidou, A., Delivanis, D.-A., Sismanopoulos, N., Zhang, B., Asadi, S., Vasiadi, M., Weng, Z., Miniati, A., et al. (2012). Mast cells and inflammation. Biochim. Biophys. Acta BBA - Mol. Basis Dis. *1822*, 21–33.

Veatch, S.L., and Keller, S.L. (2003). Separation of liquid phases in giant vesicles of ternary mixtures of phospholipids and cholesterol. Biophys. J. *85*, 3074–3083.

Verkleij, A.J., Zwaal, R.F., Roelofsen, B., Comfurius, P., Kastelijn, D., and van Deenen, L.L. (1973). The asymmetric distribution of phospholipids in the human red cell membrane. A combined study using phospholipases and freeze-etch electron microscopy. Biochim. Biophys. Acta *323*, 178–193.

de Vries, V.C., and Noelle, R.J. (2010). Mast cell mediators in tolerance. Curr. Opin. Immunol. *22*, 643–648.

Whitlock, J.M., and Hartzell, H.C. (2017). Anoctamins/TMEM16 Proteins: Chloride Channels Flirting with Lipids and Extracellular Vesicles. Annu. Rev. Physiol. *79*, 119–143.

Zhou, L., Oh, S.Y., Zhou, Y., Yuan, B., Wu, F., Oh, M.H., Wang, Y., Takemoto, C., Van Rooijen, N., Zheng, T., et al. (2013). SHP-1 Regulation of Mast Cell Function in Allergic Inflammation and Anaphylaxis. PLoS ONE *8*, e55763.

Zhou, Y., Liang, H., Rodkey, T., Ariotti, N., Parton, R.G., and Hancock, J.F. (2014). Signal Integration by Lipid-Mediated Spatial Cross Talk between Ras Nanoclusters. Mol. Cell. Biol. *34*, 862–876.

Zhou, Y., Wong, C.-O., Cho, K. -j., van der Hoeven, D., Liang, H., Thakur, D.P., Luo, J., Babic, M., Zinsmaier, K.E., Zhu, M.X., et al. (2015). Membrane potential modulates plasma membrane phospholipid dynamics and K-Ras signaling. Science *349*, 873–876.

Zhou, Y., Prakash, P., Liang, H., Cho, K.-J., Gorfe, A.A., and Hancock, J.F. (2017). Lipid-Sorting Specificity Encoded in K-Ras Membrane Anchor Regulates Signal Output. Cell *168*, 239–251.e16.

Zwaal, R.F.., Comfurius, P., and Bevers, E.M. (2004). Scott syndrome, a bleeding disorder caused by defective scrambling of membrane phospholipids. Biochim. Biophys. Acta BBA - Mol. Cell Biol. Lipids *1636*, 119–128.

Vitae

Eric Joseph Malmberg was born in Torrance, Ca on November 20, 1990. He graduated from Capital High School in 2009 in Helena, MT and attended Penn State University, double majoring in Immunology and Infectious Diseases, and Toxicology and graduated in 2013 with two Bachelor of Science Degrees. In August 2015, he entered the graduate program at the University of Texas Graduate School of Biomedical Sciences.